REPORT NO. DOT-TSC-FRA-71-7

PROGRESS ON RAM WING AT TSC WITH EMPHASIS ON LATERAL DYNAMICS

TIMOTHY M. BARROWS
TRANSPORTATION SYSTEM CENTER
55 BROADWAY
CAMBRIDGE, MA. 02142

transpo 72
U.S. International Transportation Exposition
Dulles International Airport
Washington, D.C.
May 27-June 4, 1972

JUNE 1971
TECHNICAL REPORT

Prepared for
DEPARTMENT OF TRANSPORTATION
FEDERAL RAILROAD ADMINISTRATION
WASHINGTON, D. C. 20590

The contents of this report reflect the views of the Transportation System Center which is responsible for the facts and the accuracy of the data presented herein. The contents do not necessarily reflect the official views or policy of the Department of Transportation. This report does not constitute a standard, specification or regulation.

1. Report No.	2. Government Accession No.	3. Recipient's Catalog No.
DOT-TSC-FRA-71-7		

4. Title and Subtitle	5. Report Date
PROGRESS ON RAM WING AT TSC WITH EMPHASIS ON LATERAL DYNAMICS	June 1971
	6. Performing Organization Code
7. Author(s) Timothy M. Barrows	8. Performing Organization Report No.
9. Performing Organization Name and Address Department of Transportation Transportation Systems Center 55 Broadway, Cambridge, MA 02142	10. Work Unit No. R2304
	11. Contract or Grant No. RR207
12. Sponsoring Agency Name and Address Department of Transportation Federal Railroad Administration Washington, D.C. 20590	13. Type of Report and Period Covered Technical Report for Sept. 1970 to June 1971
	14. Sponsoring Agency Code

15. Supplementary Notes

16. Abstract

Theoretical and experimental efforts conducted at TSC in the ram wing program are described. Glide Tests were performed using a simple ram wing model operating in an open rectangulat trough 50 feet long. Lift drag ratios of 13 were recorded, and a low-frequency roll oscillation was observed. A theorectical model for a flat-plate airfoil in a rectangular trough of infinite depth is described and compared with existing theories and experimental data. The lateral dynamics of tracked vehicles of this type are reviewed and the most important stability parameters are identified.

It is recommended that future research continue to focus on lateral dynamics and that careful experimental measurements be made for the stability derivatives.

17. Key Words	18. Distribution Statement
Ram Wing Ground Effect Lateral Dynamics	Availability is Unlimited. Document may be Released To the National Technical Information Service, Springfield, Virginia 22151, for Sale to the Public.

19. Security Classif. (of this report)	20. Security Classif. (of this page)	21. No. of Pages	22. Price
Unlimited	Unlimited	69	

TABLE OF CONTENTS

LIST OF ILLUSTRATIONS

LIST OF ILLUSTRATIONS (Cont)

I INTRODUCTION

The Office of High Speed Ground Transportation is presently investigating a number of methods for supporting a vehicle travelling in a high speed guideway. Of these the concept of using a fluid for suspension is among the most promising. Fluid suspension systems fall into two categories; the air cushion in its various forms, and the ram wing, which uses simple aerodynamic forces from forward speed effects to lift and guide the vehicle. The ram wing offers many advantages in terms of simplicity, reliability, reduced power requirements, and low noise levels; it therefore deserves a place in the overall research program of the Department of Transportation. The Transportations Systems Center (TSC) thus undertook a nine-month study of the potentials of this type of suspension, with a goal of demonstrating the technical advantages and disadvantages of this concept. A second purpose to this study was to establish the direction of future research on ram wing vehicles.

A fair amount of analytical work and preliminary studies have been done on ram wings which has shown the theoretical advantages of an aerodynamic type of suspension. However, it has proven quite difficult to design a vehicle which retains these advantages while not incurring any counteracting disadvantage. Several designs for ram wing vehicles have been

submitted to OHSGT. Typically the design implies a guideway of excessive width, or one that is expensive and difficult to construct. Also, it often turns out that the vehicle has a very large surface area, so that the theoretical savings in power required for lift are counteracted by an increase in parasite drag. Finally, investigators very often propose studying a particular vehicle configuration without first applying sufficient analysis in the selection of guideway cross-section: an acceptable stability analysis is often lacking. The present study is aimed at addressing some of these problems.

A first interest in evaluating any new transportation concept is to design an optimized system, which under favorable circumstances may be done using the techniques of systems analysis. Unfortunately these techniques require a considerable amount of knowledge of the operational characteristics of the components of the system as a function of the system parameters. In the case of the ram wing, knowledge of this nature is lacking, and the systems analyst is at a loss to provide any meaningful insight into the design problem. In this situation the most rational procedure is to establish a baseline configuration and perform sufficient analysis to make preliminary estimates of the operating characteristics of this design. Using these as a standard, one can then determine whether any proposed alternative design has better or worse characteristics, and if better it can be used as a new baseline. In this way one can expect

the baseline design would eventually move toward an optimum system. However, it is also apparent that the efficiency of the whole process is greatly increased if the original baseline is chosen judiciously, with appropriate attention being paid to all the features of the system which have a direct influence on eventual acceptability such as power consumption, guideway cost, safety, system capacity, etc. The evaluation made in some of these categories may of necessity be qualitative or intuitive, but it is important that items which are hard to quantify in a preliminary study, such as safety, are not completely overlooked in favor of those which are easy to quantify, such as power consumption.

The subject of stability should definitely enter into the selection of an appropriate baseline configuration and, in fact, may turn out to be an overriding consideration, as is the case in aircraft design, since the stability characteristics determine the response to guideway irregularities, and construction tolerances have a major influence on guideway cost. Enough is known about longitudinal dynamics to make an analysis of simplified baseline configurations, and to make a preliminary choice of those vehicle dimensions which apply most directly to these motions. However, very little is known about lateral stability, which is a somewhat broader and more difficult subject since the analysis varies widely with different vehicle-guideway cross sections. This results in a classic

design situation: the guideway can't be chosen until a good deal is known about lateral stability, and a stability analysis can't be done until a guideway is chosen. The remarks made on the design of the entire system apply with particular relevance to the lateral dynamics. It would be desirable to have a comprehensive study that would show the range of guideway and vehicle dimensions which lead to acceptable operational characteristics. Unfortunately it is very difficult to make such a study meaningful since many factors external to the subject of stability enter into the analysis; none of these lend themselves to easy quantification. Therefore, the study of lateral stability made at TSC, which may be found in Appendix B, was of the simplest and broadest nature. In this way it was hoped that the greatest insight into the design problem could be gleaned for a given amount of effort. A thorough and complete stability analysis is only justified when the cross sectional geometry of the guideway is more clearly established.

The experimental effort at TSC was also of a very preliminary nature, and of necessity the program was limited to a specific configuration. A glide test facility was constructed which consisted of a trough-shaped guideway one foot wide and fifty feet long, placed at an incline. A vehicle model was catapulted onto the upper end and glided in free flight to the lower end, with lift, drag, and stability being observed. The purpose of these tests was to establish the overall performance

of the candidate vehicle configuration and to identify the most important stability problems. An equally important function was the simple demonstration of a ram wing concept. One of the reasons the ram wing has received so little attention in comparison to pressurized air cushions is the fact that almost no hardware exists which utilizes this concept. It is hard to justify expenditure for research on a concept which only exists on paper and in the minds of aerodynamicists. The expectation was that a good model demonstration of a ram wing would allow a more meaningful evaluation of its advantages relative to alternative methods of suspending high speed ground transportation vehicles.

One of the major ingredients in designing the models used in the glide tests was simple intuition. This turned out to be acceptable for the type of test conducted, but a rational design procedure for full scale vehicles can only be established on the basis of a more scientific and fundamental process. A theoretical model of the flow underneath a ram wing in a trough was therefore developed, which appears in Appendix A. With some additional development this analysis may be used to predict stability coefficients for a wide variety of vehicle-guideway configurations; once this can be done with confidence the required design process can be established.

II PROGRAM SUMMARY

This chapter summarizes the results of the theoretical and experimental investigations conducted at TSC in the nine months from October 1, 1970 to June 30, 1971. It was felt that a short description of the various aspects of the program would be most appropriate here, detailed calculations and experimental data occur in the appendices.

EXPERIMENTAL PROGRAM

The general shape of the model used in the glide tests is shown in Fig. 2-1. It consists of a main wing with a canard in the front which provides longitudinal stability. Both the canard and the main wing have integrated lateral surfaces which were intended to provide lateral stability. The canard is mounted in such a way that its angle of attack relative to the main wing can be set to any desired value, between certain limits, for a given test flight.

The selected configuration flies very much as expected at a clearance of about one half inch above the bottom of the trough. The longitudinal stability is excellent. It was originally intended that stability derivatives could be obtained by varying the angle of the canard and noting the effect on the flight attitude. However, the longitudinal stability was so strong that very little change in flight attitude was noted even though the incidence of the canard was varied through ten degrees. The longitudinal arrangement was based on theory for

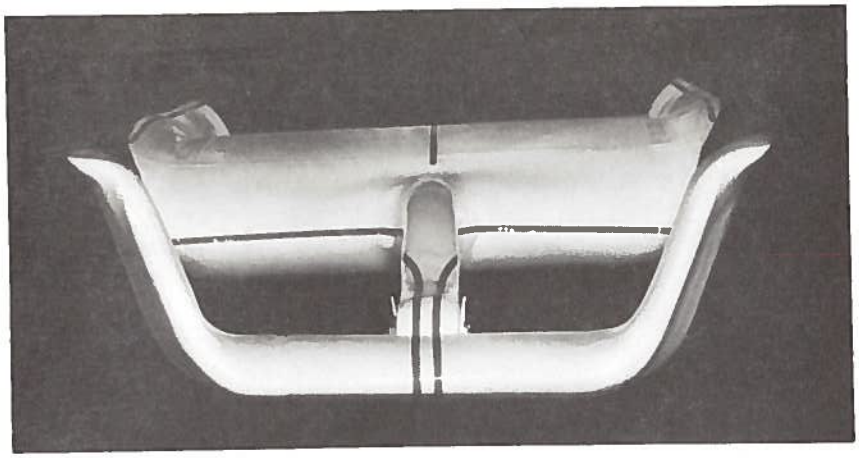

Front View

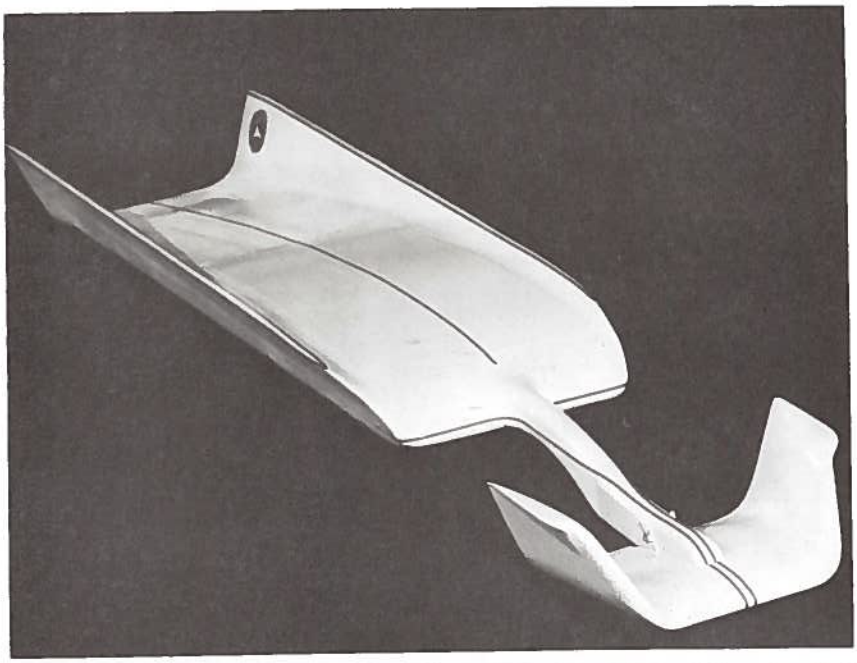

3/4 View

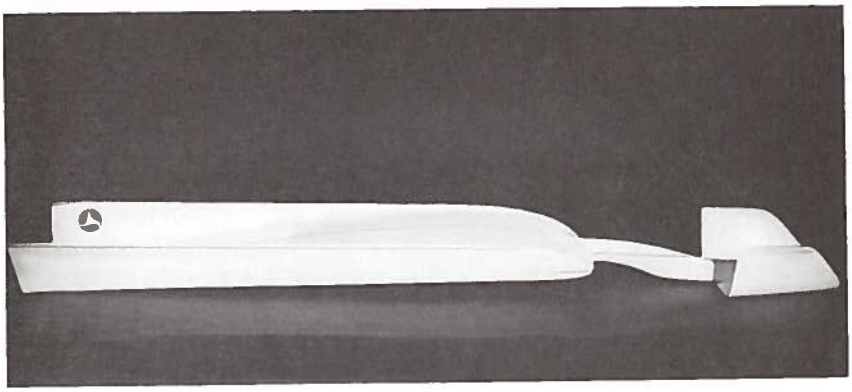

Side View

Figure 2-1. Model Configuration

two-dimensional wings in ground effect, whereas some very significant three-dimensional effects were evidently adding to the pitch stability. It might even be possible that a design which fully exploits these effects could eliminate the necessity of a canard altogether.

The lateral behavior of the model proved to be quite interesting. Although it shows a definite static side stability, there is a dynamically coupled roll-sway oscillation which takes place as the model moves down the track. About one and a half cycles of this oscillation take place in the fifty foot length of test guideway. This oscillation is similar to the type which is predicted from the simple analysis in Appendix B.

In the original series of tests the sides of the guideway were vertical, forming a rectangular trough, while the model had sides with a slope of 20°, with respect to the vertical as shown in Fig. 2.1. Although the model flew successfully in this track the lateral motions were large and the vertical clearances were small and uneven. The track was therefore modified to conform more closely to the shape of the model. This increased the vertical clearance and reduced the lateral motions, although some oscillation persisted.

The instrumentation of these glide tests was not constructed until after the above change in track configuration was made. It consists of vertical slits cut on each side of the track as shown in Fig. 2-2. A parallel beam of light shines through the slits and into a photocell. As the model flies by the slits it

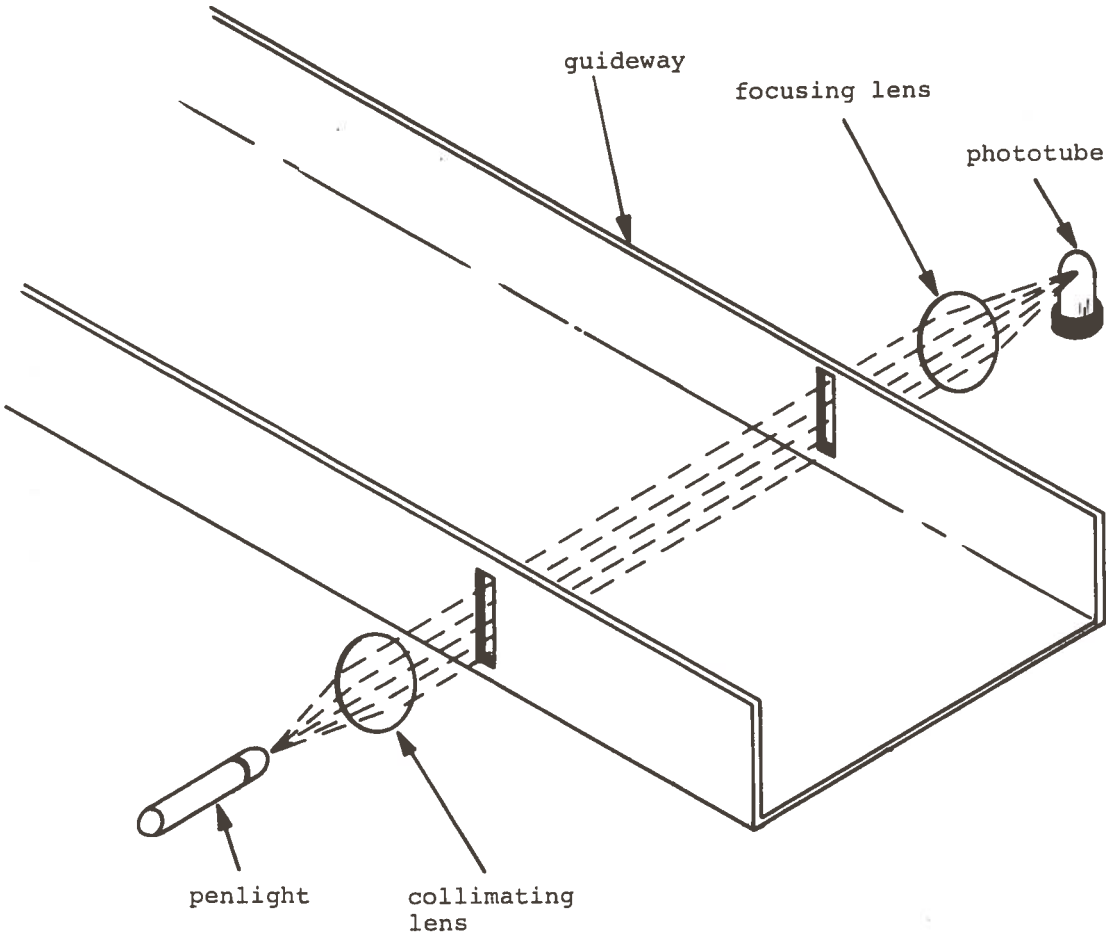

Figure 2-2. Guideway Instrumentation. As the Model Passes Between the Slits it Blocks Off Part of the Light. The Clearance is Proportional to the Remaining Portion of Light which Passes Under the Model.

blocks off a portion of the light, and the photocell gives a current output proportional to the light that passes under the model. This output is thus a measure of the vertical clearance. By taking the difference in height between the leading and trailing edges of the model, the angle of attack can be calculated. Finally, the total time required for the model to pass by the slit gives a measure of the velocity. A total of three such optical systems were placed along the length of the track, and the output of each was recorded on an oscillograph. In this way the height, angle of attack, and velocity could be recorded at three separate points during each test.

It turned out that the velocity measurement was by far the most useful for the tests performed during this preliminary program. Significant results were not obtained from the other measurements due to interference from the above mentioned rolling motions. It was possible to determine that the clearance at the trailing edge was approximately one half inch, but very little additional information could be determined. Hopefully, future models can be designed which do not have a roll problem, in which case more significant height measurements can be made. Also, a technique is currently being developed to measure roll angle optically. If this proves successful it will greatly increase the usefulness of the height and angle of attack data.

The velocity measurements were used to give a measure of acceleration, with this known it is a simple matter to compute

the drag coefficient. A lift-drag ratio of 13 was measured at a lift coefficient of 0.7. These values are both comparable to what might be expected on a full scale vehicle. Higher values of L/D can be achieved if the gaps around the sides of the vehicle are reduced.

High speed films were taken of the flying ram wing model which proved to be a very useful check on the guideway instrumentation. The roll oscillations could be clearly observed and it was verified that the vertical clearances were indeed in the same range as those calculated from the optical measurements. Two frames from one of these films which show the extreme left and right roll angles may be found in Fig. 2-3.

Although these films give a very useful view of the overall flight characteristics of the model, they are quite expensive and not convenient for taking quantitative data. Thus, they cannot be used to serve the same function as the guideway instrumentation. It is anticipated that future tests will involve some films of each new model configuration, but that the bulk of the test data will come from other means.

THEORETICAL INVESTIGATIONS

A model for the flow about a rectangular plate in a trough was formulated and a solution was obtained which appears in Appendix A. Basically this solution is a modification of the two-dimensional model reported in Reference 1 which allows for some flow through the side gaps. The effect on the pressure

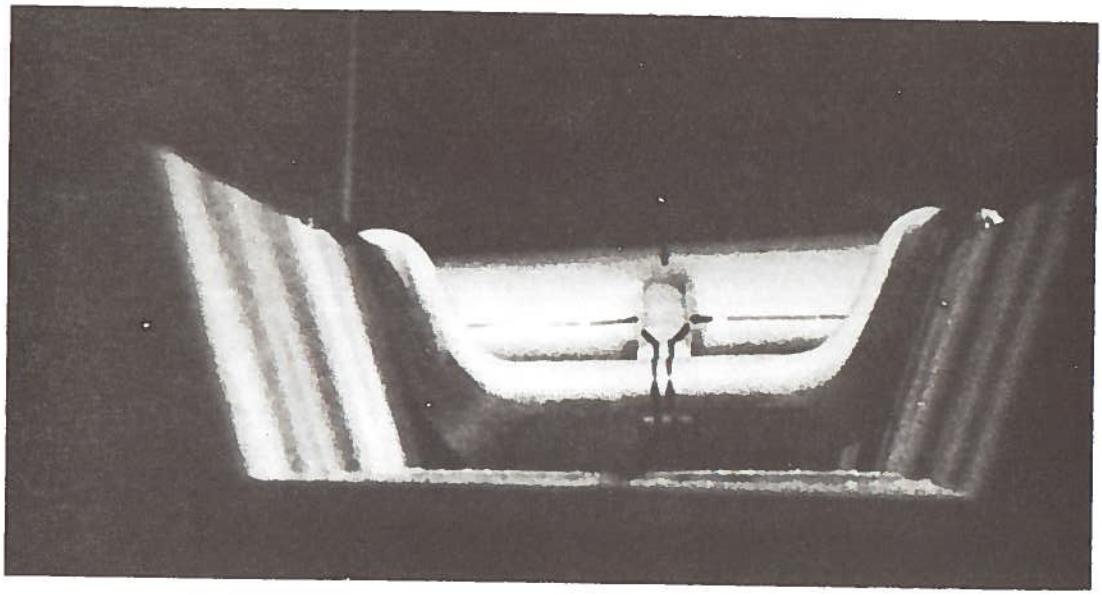

(a) Left Roll

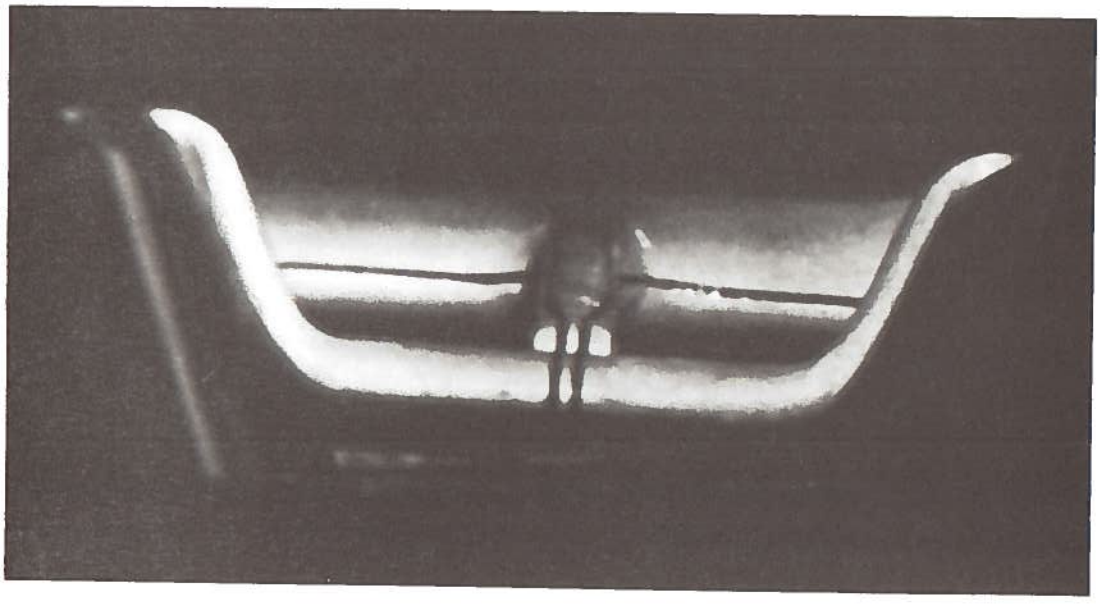

(b) Right Roll

Figure 2-3. Head-on View of the Flying Model in the Glide Track. These Pictures are taken from High Speed Movies and Show Both Extremes of Roll Angle.

distribution of even fairly small gaps can be quite dramatic, especially if the lifting surface is of low aspect ratio. It is very likely that the flow through the gaps will deviate appreciably from the given potential flow solution at the higher angles of attack, and a simple model is presented which can predict the gross effects of viscosity on the pressure distribution.

The potential solution gives good agreement with other aerodynamic theories for the limiting cases of very large and very small aspect ratios. It needs some further development before it can be used to predict stability coefficients. Once this is done and satisfactory agreement is obtained with experiment, analyses of the free flight dynamics of ram wing vehicles can be conducted with some confidence.

A limited amount of insight can be obtained from a dynamic analysis even if the stability coefficients are unknown. Appendix B gives a very general study that shows which of the lateral stability coefficients are most important. Further results of this analysis follow.

GENERAL CONCLUSIONS TO DATE

It was felt that this program was quite fruitful in providing insight into the potential performance of ram wing vehicles and in establishing a program which will eventually yield the technical background necessary to design a full scale vehicle.

Although the ram wing may offer many advantages in terms of simplicity and low power requirements, certain difficulties in achieving sufficient lateral stability have been identified. These may be summed up in the following two main points:

1. Using realistic values for the width of the guideway (i.e. 12 feet maximum) it is very difficult to obtain adequate roll stiffness.
2. If aerodynamic forces are used to both lift and guide the vehicle, there is a strong probability of an unstable coupling between roll motions and side sway motions, unless appropriate features are incorporated into the design of the vehicle itself.

Of these two problems, the first is certainly the most serious, as it appears to have no solution which doesn't involve some cost. It may turn out that some kind of active roll control is necessary, possibly by activating a pair of differential flaps at the trailing edge. With regard to roll-sway coupling, it is felt at this time that with sufficient additional knowledge of lateral dynamics the stability problem can always be solved without a significant cost penalty.

The ram wing is at its greatest advantage if the operating clearance is large enough to make a secondary suspension system unnecessary. At this point it appears that vertical clearances of this magnitude are achievable, but for good operating performance comparatively small gaps are required on the sides,

which will probably necessitate some kind of flexible sealing arrangement to accomodate the lateral motions. A full scale ram wing vehicle may thus look very much like current tracked air cushion designs, with the possible addition of some kind of stabilizing surface either ahead of or behind the main body. The major difference would be the lack of compressors and supply ducts for the cushions.

The glide test is a useful technique for demonstrating the overall flight characteristics and performance of ram wing configurations, but it does have its limitations. Since all the dynamic effects are occurring simultaneously, it is often difficult to separate the individual effects. It would be ideal to have a facility in which the forces and moments could be measured as the orientation of the model is varied in a controlled fashion. The recommended techniques for doing this are discussed in the next chapter.

III RECOMMENDATIONS FOR FUTURE RESEARCH

Although the glide tests conducted during this program involved a specific guideway geometry, it is the desire of the government to remain open to all possible configurations during the search for an optimum system. The comments made in the introduction are here re-emphasized. A major determinant of the desirability of a transportation system is the response of the vehicle to guideway irregularities and crosswinds, which is intimately related to the question of stability. The longitudinal dynamics are mainly determined by the configuration of the vehicle itself, but the lateral dynamics, on the other hand, are a function of the guideway cross-section. Thus a research program which continues to emphasize lateral dynamics should lend the greatest insight into what a ram wing guideway should look like. Once this is determined the analysis and design of the vehicle may proceed with a great deal more focus.

A systematic design procedure for these vehicles must rest on a solid foundation of theory and experiment. A survey of several possible experimental techniques is now being conducted jointly between MIT and TSC; a very brief summary of the results of this effort is worthwhile here. The analysis of the dynamics of a ram wing may proceed as diagrammed in Fig. 3-1, which shows how the various testing techniques become useful at different stages of the analysis. The first prerequisite is to obtain

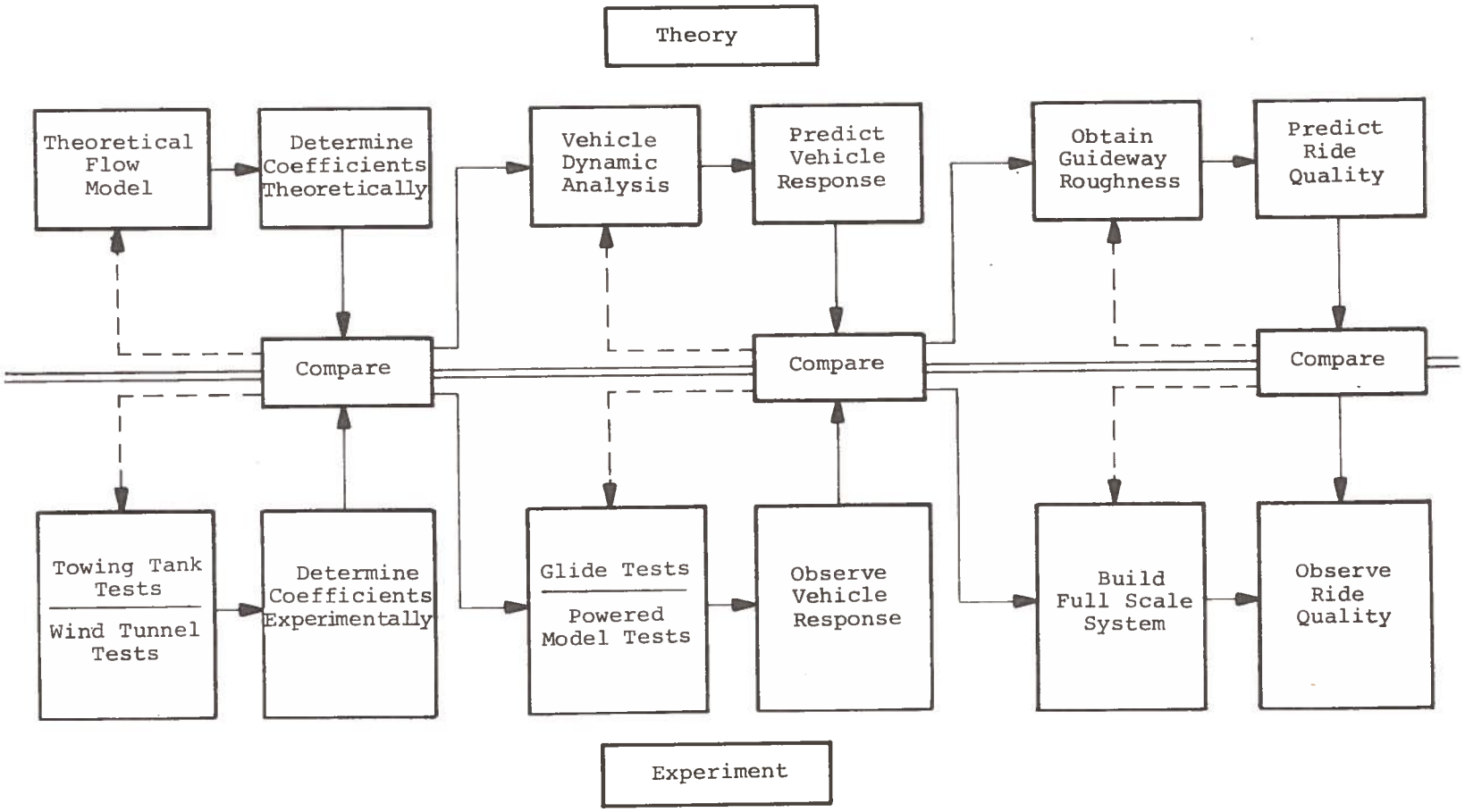

Figure 3-1. Ram Wing Development Program

the stability coefficients; the best experimental methods to do this involve either a fixed model (in a wind tunnel) or one which is held in a carriage. The wind tunnel has many difficulties with simulating the relative motion between the vehicle and the guideway. With a carriage, on the other hand, it is difficult to achieve sufficient velocity through the air to produce measurable forces, but if water is substituted for air as a fluid medium, this problem is negated, at a cost of some technical difficulties with instrumentation. On the whole it appears that the towing tank offers the most viable technique for obtaining stability derivatives, and this is the method which is planned at TSC during the next fiscal year.

A wind tunnel technique which could properly simulate the relative vehicle-guideway motion would have certain advantages over a towing tank. Higher Reynolds numbers are possible and it is more convenient to get pressure data. The possibilities for doing this will continue to be investigated, but there are presently no detailed plans for experiments of this nature. These will depend on further development of facilities between TSC and MIT.

Once adequate agreement is found between theory and experiment for the stability coefficients, a vehicle dynamic analysis can be performed, which can be checked experimentally using glide tests or powered model tests. It is hoped that the instrumentation for the present glide test track can be more

fully developed so that more useful information can be obtained from this facility, which will serve as a very practical complement to the towing tank.

Powered model tests are very expensive and require a great deal of sophisticated instrumentation to obtain useful data. Although they provide the best simulation of a full scale system and can serve as a dramatic demonstration, they should not be attempted until the flight characteristics of a particular configuration are demonstrated by glide tests. Once this is done, however, a good series of powered model tests can be a very useful technique for advanced development. It is really the only method by which such features as curves and switches can be studied. Also, the problem of crosswind gusts could be examined most effectively with this type of testing.

One area which deserves special mention is active suspension systems. It should be apparent that the ram wing is particularly amenable to active control, since a small change in the flow conditions at the trailing edges can produce a huge force over a large area of the undersurface. Such changes may be induced by a mechanical flap, as on conventional aircraft, or by a jet flap.

If optimal control theory is used to design the devices which direct the suspension forces on the vehicle, the ride quality should be quite independent of the particular method which is used for the primary suspension. That is, the ram

wing in this situation will give comparable ride quality to the air cushion or even wheeled vehicles, given that the guideway roughness and suspension stroke length are the same. Thus it can be seen that if active suspension becomes an accepted technique for ground transportation, the potential ride quality attainable by any particular method of primary suspension will no longer serve as a basis for comparison between methods. What is important, however, is the ease by which an optimal control strategy can be implemented, and in this regard the ram wing has a slight edge over the air cushion and both have a significant advantage over the wheel. (If this aspect is used as the sole criterion for judging suspension concepts, in view of the current highly developed state of electronic technology it is possible that magnetic suspension has the edge over all three.)

The subject of active control immediately brings up the question of reliability. Most likely it will be desirable to design a vehicle which has basic stability in all degrees of freedom, and to use active control to upgrade the ride quality. This is where the emphasis in the ram wing program presently lies - in finding configurations which have basic stability (and hopefully passable ride quality). Even with such a design, however, it is highly advantageous to use active devices with a maximum of reliability and low maintenance cost. Current aircraft practice in active control is to use electronic circuitry to drive hydraulic actuators. However, in the case of ground

transportation it may turn out that relatively simple logic will provide adequate ride quality; if this is the case fluidic devices can provide an excellent means for performing the necessary functions. This is especially likely if a viable sub-optimal control scheme can be found. The attractiveness of this concept is further enhanced by the fact that fluidic devices are quite capable of sensing acceleration, roll rates, position, and other information needed for active suspension. Thus the electrical interface can be avoided entirely. Furthermore, if a jet flap is used to implement the control logic, it may even be possible to eliminate any mechanical interface. The ram wing would thus retain its major advantage of having no moving parts, even though actively controlled.

There are two important points to be drawn from this discussion:

1. Further studies of active control, and in particular fluid control devices, are certainly warranted.
2. In the search for an optimum guideway cross-section, with active control the stability aspects of the design are less important than they are in the case of a totally passive suspension. This means that more attention can be paid to the civil engineering aspects of the design, resulting in lower cost.

In conclusion, it can be seen that a great deal of fundamental research is required before a meaningful systems analysis and design can be accomplished. A start can be made on obtaining this knowledge using existing experimental facilities such as the wind tunnel and the towing tank. New testing techniques will have to be developed and eventually new types of facilities may have to be constructed before the ram wing concept will result in practical hardware.

REFERENCES

1. Ashill, P.R., 1970, "On the Minimum Induced Drag of Ground-Effect Wings" Aeronantical Quarterly Vol. XXl, No. 3, p. 211.

2. Ashley, H. and Landahl, M., 1965, Aerodynamics of Wings and Bodies, Reading, Massachusetts: Addison Wesley.

3. Barrows, T.M. and Widnall, S.E., 1970, "Optimum Lift-Drag Ratio for a Ram Wing Tube Vehicle", AIAA Journal, Vol. 8, p. 491.

4. Barrows, T.M., Widnall, S.E., and Richardson, H.H., 1970, "The Use of Aerodynamic Lift for Application to High Speed Ground Transportation", PB 197 242.

5. Frederick, D.K. and Lee, I., 1967, "Roll Control of a Fluid-Supported Vehicle Moving in a Nonevacuated Tube", ASME paper 67-TRAN-8.

6. Gallington, R.W., Miller, M.K., and Smith, W.P., 1971 "The Ram-Wing Surface Effect Vehicle: Comparison of One-Dimensional Theory with Wind Tunnel and Free Flight Results" Frank J. Seiler Research Lab report No. SRL-TR-71-0012, USAF Academy.

7. Kaario, T. J., 1935, "Process for Eliminating Friction Between a Surface Vehicle and the Surface", Finnish Patent No. 18630.

8. Munk, M., "The Minimum Induced Drag of Airfoils" NACA Rept. 121.

9. Peppin, J., 1970 "The Study of a Ram Wing in a Trough" M.S. Thesis, MIT (Unpublished)

10. Widnall, S.E., and Barrows T.M., 1970, "An Analytic Solution for Two and Three Dimensional Wings in Ground Effect", Journal of Fluid Mechanics, Vol. 41, p. 769.

NOTE: Reports with PB prefixes can be obtained from the National Technical Information Service (NTIS), Springfield, Virginia 22151.

APPENDIX A

THEORETICAL FLOW MODEL FOR A FLAT PLATE
IN A RECTANGULAR TROUGH

APPENDIX A

THEORETICAL FLOW MODEL FOR A FLAT PLATE IN A RECTANGULAR TROUGH

In a recent paper Widnall and Barrows (1970) reviewed the ground effect phenomena and analyzed a new class of problems in which the clearance of the wing is very small using the method of matched asymptotic expansions. The particular case of a flat surface of elliptical planform operating over an infinite ground plane was investigated in detail. It was shown that this wing generated an optimal spanwise distribution of lift. Although a configuration related to this shape might find possible use in certain instances, such as a vehicle designed to travel over water, for application to high speed ground transportation the general idea of a wing in a trough holds much more promise. Not only do the sides of the trough increase the lifting efficiency, but they protect the vehicle from cross winds, and in addition if the guideway is to be elevated they may present structural advantages.

A flat wing in a rectangular trough is of course the simplest case to analyze and shows the basic aerodynamic characteristics of this type of configuration. This problem could be studied using conventional computer techniques such as a distribution of horseshoe vortices, but this would overlook the basic simplicity of the problem and it would be unclear how to modify the analysis if a more complicated cross-section were chosen. The basic advantage of the present asymptotic technique

is that it divides the flow into several regions, each of which is analyzed separately, thus explicitly revealing the nature of the flow field in each area and allowing a great deal of flexibility. If the geometry of any of the regions is varied the appropriate analysis may be modified in that part, and the only change to the remainder of the flow is a change in the matching conditions.

The most successful analytic techniques in aerodynamics reduce a given three-dimensional flow to a two-dimensional problem through a suitable emphasis of one of the coordinates. Such is the case with lifting line theory and slender body theory. In the present problem the flow is divided into three regions, in each of which the flow may be closely approximated by a two-dimensional solution. The coordinates are shown in Fig. A-1, which shows a flat plate in a trough with sides which extend upward to infinity. We have:

1. The channel flow, in the narrow region between the wing and the ground. With the condition that the clearance is very small, perturbations in the vertical direction become an order of magnitude smaller than the horizontal perturbations, so that this flow may be described in the x-y plane.
2. The edge regions. It can be shown that near the side edges the x-perturbation is very small. Because of the gap between the wing and the trough, however, the

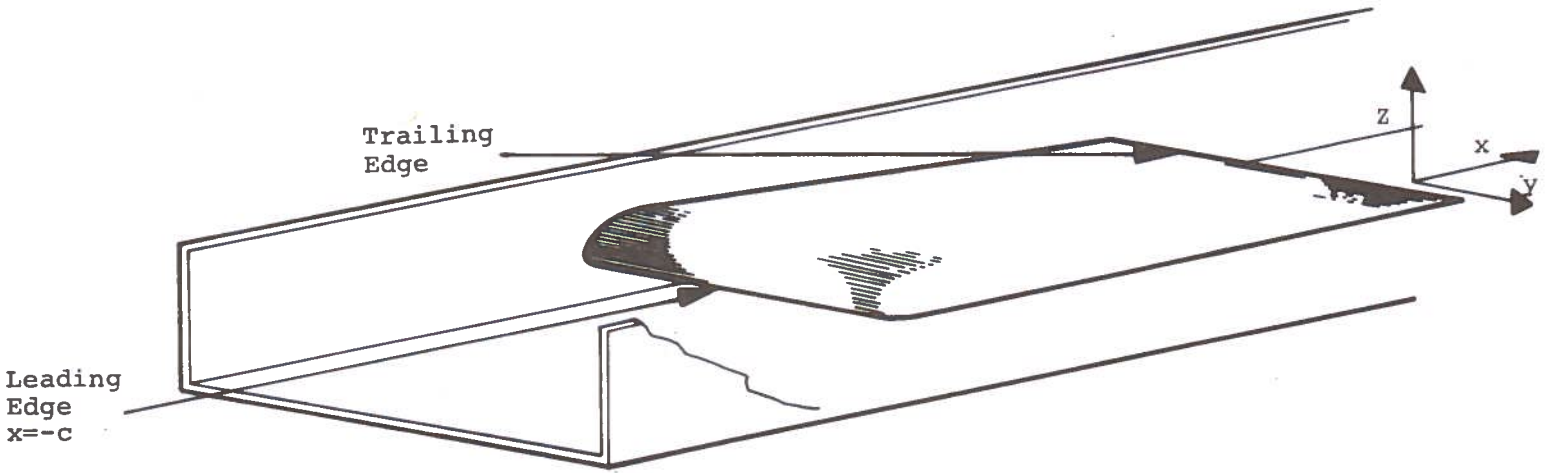

Figure A-1. Coordinate System for a Ram Wing in a Trough.

z-perturbation becomes important, and so this flow is best described in the y and z coordinates, i.e. the cross flow plane.

3. The outer flow. In the external field, because of the confining nature of the walls of the trough, the y pertubation is suppressed and the flow may be described in the x-z plane.

THE TREFFTZ PLANE

The manner in which these flows are joined together is best introduced by first considering the flow far downstream of the wing, such that the x-perturbations may be neglected. Thus in a cross flow plane we have the picture shown in Fig. A-2 in which all lengths have been normalized by the semispan.

Certain basic information may be found when the velocity potential ϕ in the Trefftz plane is known. The discontinuity in ϕ across the wing is equal to the bound circulation, as has been shown by many authors (see for example Ashley & Landahl 1965):

$$\phi_{upper} - \phi_{lower} = \Gamma(y) \qquad (1)$$

Of greatest interest is the case in which $\Gamma(y)$ is distributed in a manner which gives a minimum of induced drag. For a planar wing in a free stream, Munk (1921) showed that a necessary condition for this optimum distribution is that the downwash be constant across the span. It is most convenient to

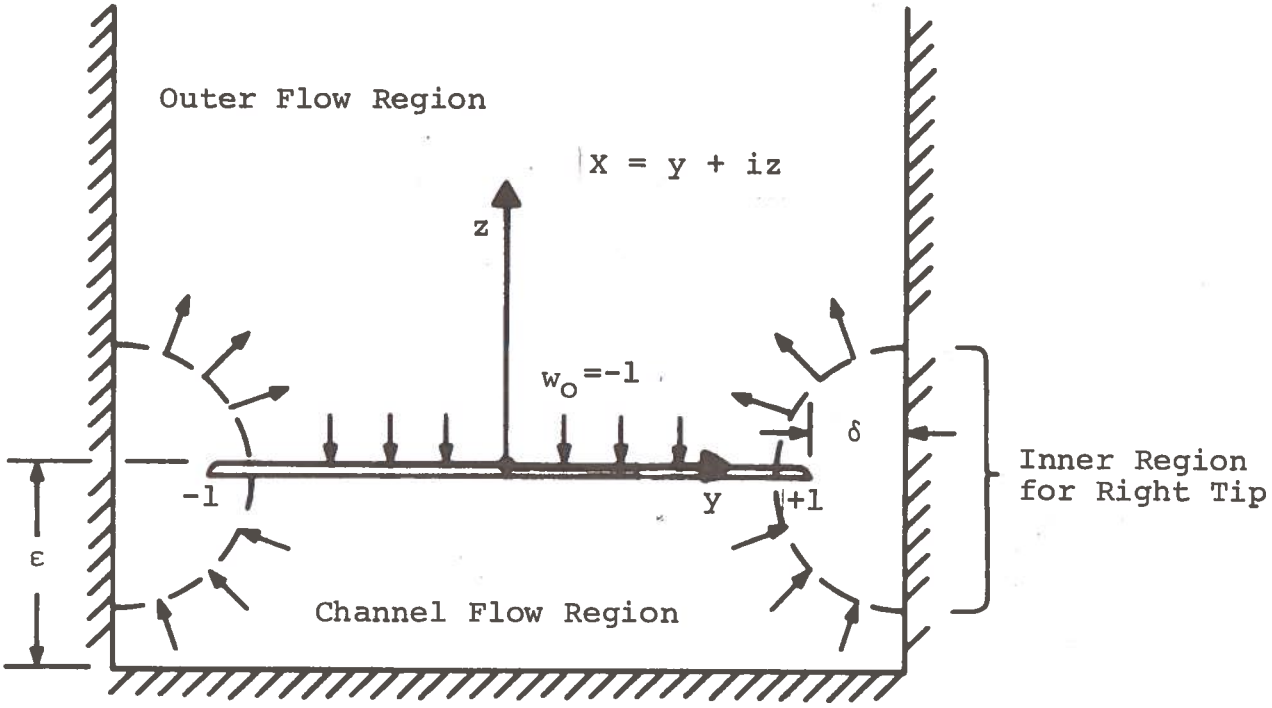

Figure A-2. Trefftz Plane for a Ram Wing in a Rectangular Trough of Infinite Depth

calculate the induced drag using a notation introduced by Cone (1962).

$$C_{D_i} = \frac{C_L^2}{\pi\ K\ AR}$$

where K is the aspect ratio augmentation factor which can be computed from

$$K = \frac{1}{\pi\ w_o} \int_{-1}^{+1} \Gamma(y)\,dy \qquad (2)$$

Here w_o is the downwash at the wing, taken as unity throughout this section. The quantity K AR is known as the effective aspect ration and is a basic figure of merit for a lifting system. Barrows and Widnall (1970) showed that all these formulas are valid for the case of wings near solid boundaries, and went on to investigate the case of a wing at a small clearance ε above an infinite ground plane. The following simple approximation for the optimum distribution was found:

$$\Gamma(y) = \frac{1-y^2}{2\varepsilon} \qquad (3)$$

The purpose of this section shall be to examine how this distribution changes when the flow around the ends of the wings is restricted by the walls of the trough.

THE CHANNEL FLOW

The coordinate system for the Trefftz plane is shown in Fig. A-2.

Let $X = y + iz$

and $q^c = v - iw$ (4)

be complex velocity. For unit downwash at the wing our boundary condition reads: $v = -1$ at $z = 0$, $-1 < y < +1$.

We make the stipulation that the wing operates at a small vertical clearance and has an even smaller clearance δ at the sides:

$$\delta << \varepsilon << 1 \ . \tag{5}$$

In the limit as $\delta \to 0$ the flow near the gap between the side of the trough and the wing becomes that of an ideal sink. To represent this flow one could place a sink at each wingtip plus a pair of sinks at the image positions below the ground. This maintains the condition of no vertical velocity w through the ground plane. However these images would cause a non-uniform vertical flow at the wing position $z = 0$. It is more convenient to place sinks at two infinite series of image points along the walls of the trough, such that $w = o$ along all lines $z = n\varepsilon$ $(n=0,\pm1,\pm2...)$.

A constant downwash of unit magnitude is satisfied by simple corner flow, $q^c = i + X/\varepsilon$ whereas each infinite distribution of sinks may be represented by the hyperbolic cotangent. Adding these all together, we obtain for the channel flow

$$q^c = i + \frac{1}{\varepsilon}\left[X - \coth\frac{\pi(X-1)}{2\varepsilon} - \coth\frac{\pi(X+1)}{2\varepsilon}\right]$$

This satisfies the boundary conditions on the wing and the ground, and the condition at the walls, v = o at y = $\pm$ 1, is very closely approximated for any $\varepsilon < 1$. The above may be integrated to get the complex potential $F^c = \phi^c + i\psi^c$:

$$F^c = iX + \frac{X^2}{2\varepsilon} - \frac{2}{\pi} \log \sinh \frac{\pi(X-1)}{2\varepsilon} - \frac{2}{\pi} \log \sinh \frac{\pi(X+1)}{2\varepsilon} + C^c \tag{6}$$

where C^c is a constant which is to be determined. To obtain the potential on the wing we set z = o and take the real part of (6)

$$\phi^c = \frac{y^2}{2\varepsilon} - \frac{2}{\pi} \log \sinh \frac{\pi(1-y)}{2\varepsilon} - \frac{2}{\pi} \log \sinh \frac{\pi(1+y)}{2\varepsilon} + C^c \tag{7}$$

THE EDGE FLOW

In order to match the above solution to the flow in the gaps it is necessary to focus on the geometry of the edge regions. The potential here is called the "inner solution" in the usual notation of asymptotic expansions. Fig. A-3 shows a magnification of the right tip of the wing; all the external features of the flow are obscured leaving the simple problem shown. For this region we first translate to a new set of coordinates whose axes form the wing and the right wall of the trough:

$$X_r = y_r + iz_r \tag{8}$$

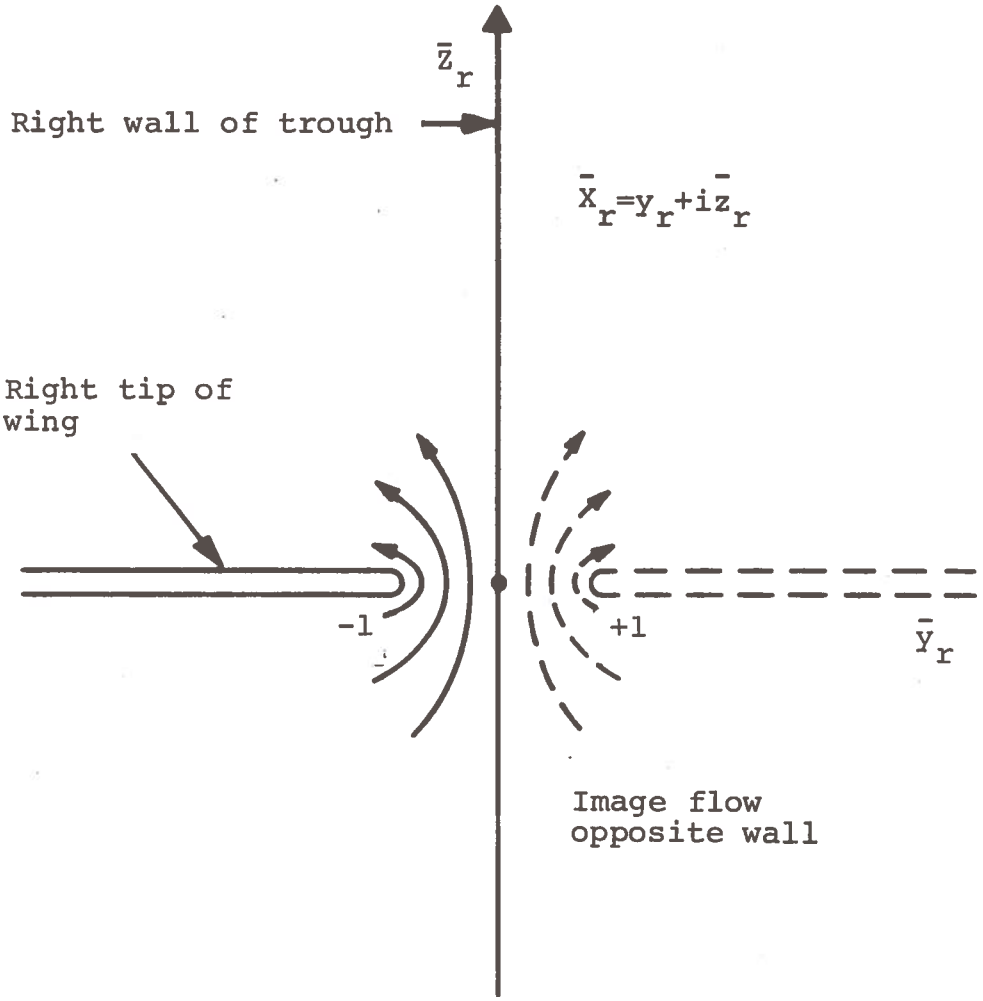

Figure A-3. The Flow in the Inner Region of the Right Wingtip

where

$$y_r = y - 1 - \delta \tag{9}$$

Next, an inner variable $\bar{X}_r$ is defined

$$\bar{X}_r \equiv X_r/\delta$$

The inner flow may be described by the well known solution for flow through an orifice, plus unit downwash:

$$q^i(\bar{X}_r) = \frac{M}{\sqrt{\bar{X}_r^2 - 1}} + i \tag{10}$$

The magnitude of this solution, M, must be chosen such that a unit volume of flow passes through the orifice in unit time; which gives

$$M = \frac{2}{\pi} \tag{11}$$

The potential on the wing may be found by integrating (10), setting $\bar{z} = 0$, and taking the real part of the resulting expression:

$$\phi^i = \frac{2}{\pi} \log \left(\bar{y}_r \pm \sqrt{\bar{y}_r^2 - 1} \right) + C^i \tag{12}$$

where C^i is, again, a constant to be determined.

In view of the branch point at $\bar{y}_r = -1$, the + is taken for the top surface of the wing and the - for the bottom. Taking the top surface limit as $\bar{y}_r \to -\infty$ gives the outer limit of the inner solution:

$$\phi^{io} = \frac{2}{\pi} \log \frac{2y_r}{\delta} + C^i \tag{13}$$

For the lower surface, as $\bar{y}_r \to -\infty$ we obtain the channel flow limit of the inner solution

$$\phi^{ic} = \frac{-2}{\pi} \log \frac{2y_r}{\delta} + C^i \tag{14}$$

These are the required limits for proper matching above and below the wing.

THE OUTER FLOW AND THE MATCHING PROCEDURE

For the outer flow, we are only interested in the upper half plane of Fig. A-2. In the limit $\delta \to 0$ the flow from the gaps approaches that of two ideal sources, of the same strength as the sinks in the channel flow solution; these are located at the wing tips, $y = \pm 1$. In order to suppress flow through the walls of the trough a system of image sources is placed at all points $y = n$, n odd. The downwash condition is satisfied by uniform vertical flow, this can be added to a mathematically simple expression for the sources to obtain the complex outer flow potential:

$$F^O = \frac{2}{\pi} \log \left[2 \cos \frac{\pi X}{2} \right] + iX \tag{15}$$

The boundary condition that $F^O \to 0$ as $z \to \infty$ is satisfied by this solution as written. We are now able to establish the inner limit of the outer solution in a straightforward fashion, setting $z = 0$, using (9), and taking the limit of the real part of (15) as $y_r \to 0$.

$$\phi^{o}(y_r) = \frac{2}{\pi} \log \left[2 \sin \frac{\pi y_r}{2} \right]$$

$$\phi^{oi}(y_r) = \frac{2}{\pi} \log (\pi y_r) \qquad (16)$$

Using the established rules of matched asymoptotic expansions ϕ^{oi} must equal ϕ^{io}, so that by comparing (13) and (16) we obtain

$$C^{i} = - \frac{2}{\pi} \log \frac{2}{\pi\delta} \qquad (17)$$

This establishes the inner solution which allows us to procede with the matching between the edge region and the channel flow. From (14) and (17) we have

$$\phi^{ic} = - \frac{2}{\pi} \log \frac{4y_r}{\pi\delta^2} \qquad (18)$$

which must equal the inner limit of ϕ^{c}. Upon inserting (8) into (7) and taking the limit as $y_r \to 0$ we obtain

$$\phi^{ci} = \frac{-3-\varepsilon^2}{2\varepsilon} - \frac{2}{\pi} \log \frac{\pi y_r}{4\varepsilon} + C^{c} \qquad (19)$$

Comparing (18) and (19) gives

$$C^{c} = \frac{3+\varepsilon^2}{2\varepsilon} + \frac{2}{\pi} \log \frac{\pi^2\delta^2}{16\varepsilon} \qquad (20)$$

which yields our final expression for the potential in the channel:

$$\phi^c = \frac{y^2+3}{2\varepsilon} - \frac{2}{\pi}\left[\log \sinh \frac{\pi(1-y)}{2\varepsilon} + \log \sinh \frac{\pi(1+y)}{2\varepsilon} + \log \frac{16\varepsilon}{\pi^2\delta^2}\right] . \qquad (21)$$

For the case of small ε we may use the following approximation

$$\frac{2}{\pi} \log \left[2 \sinh \frac{\pi(1-y)}{2\varepsilon}\right] \cong \frac{1-y}{\varepsilon} \qquad (22)$$

This is valid everywhere except for a small region of $o(\varepsilon)$ near $y = 1$. A similar approximation may be made for the term corresponding to $(1+y)$. Thus (21) may be approximated by

$$\phi^c \cong \frac{y^2-1}{2\varepsilon} - \frac{2}{\pi} \log \frac{4\varepsilon}{\pi^2\delta^2} \qquad (23)$$

A first approximation to the bound circulation may now be calculated using (1) and noting that the contribution from the outer flow is an order of magnitude smaller than either of the terms in (23). Thus

$$\Gamma(y) \cong \frac{1-y^2}{2\varepsilon} + \frac{2}{\pi} \log \frac{4\varepsilon}{\pi^2\delta^2} \qquad (24)$$

This approximation should be compared to (3), and shows explicitly that the effect of the walls is to boost the bound circulation near the tips of the wing by a factor proportional to $\log (1/\delta)$; the distribution remains parabolic near the center. For the limiting case of no gap the circulation, and hence the

lift, becomes infinite for a given amount of downwash. A better way to state this is that for a given amount of lift the downwash goes to zero like 1/log δ. Perhaps the most illustrative manner to show the implications of (24) is to compute K using (2):

$$K = \frac{2}{3\pi\varepsilon} + \frac{8}{\pi^2} \log \frac{2}{\pi\delta} + \frac{4}{\pi^2} \log \varepsilon \qquad (25)$$

which shows that the effective aspect ratio of the wing becomes infinite as either δ or ε goes to zero.

Eq. (24) is only valid in the middle region of the wing and does not properly show that $\Gamma = 0$ at the tips, as is of course necessary. To do this we must form a composite solution for ϕ as follows:

$$\phi = \phi^c + \phi^i - \phi^{ic} \qquad (26)$$

A similar formula holds for the potential above the wing with ϕ^o replacing ϕ^c. By taking the difference between these we may form a more accurate expression for Γ. Fig. A-4 shows the spanwise distribution of lift normalized by Γ_o, the circulation at the center, for several values of δ. This shows somewhat more clearly how the lift becomes constant across the span (the limiting case of a two dimensional airfoil) as the gap width goes to zero.

It is very interesting to compare the lifting efficiency predicted by (25) with the results obtained by Ashill (1970), who analyzed the Trefftz plane flow for a wing with end plates

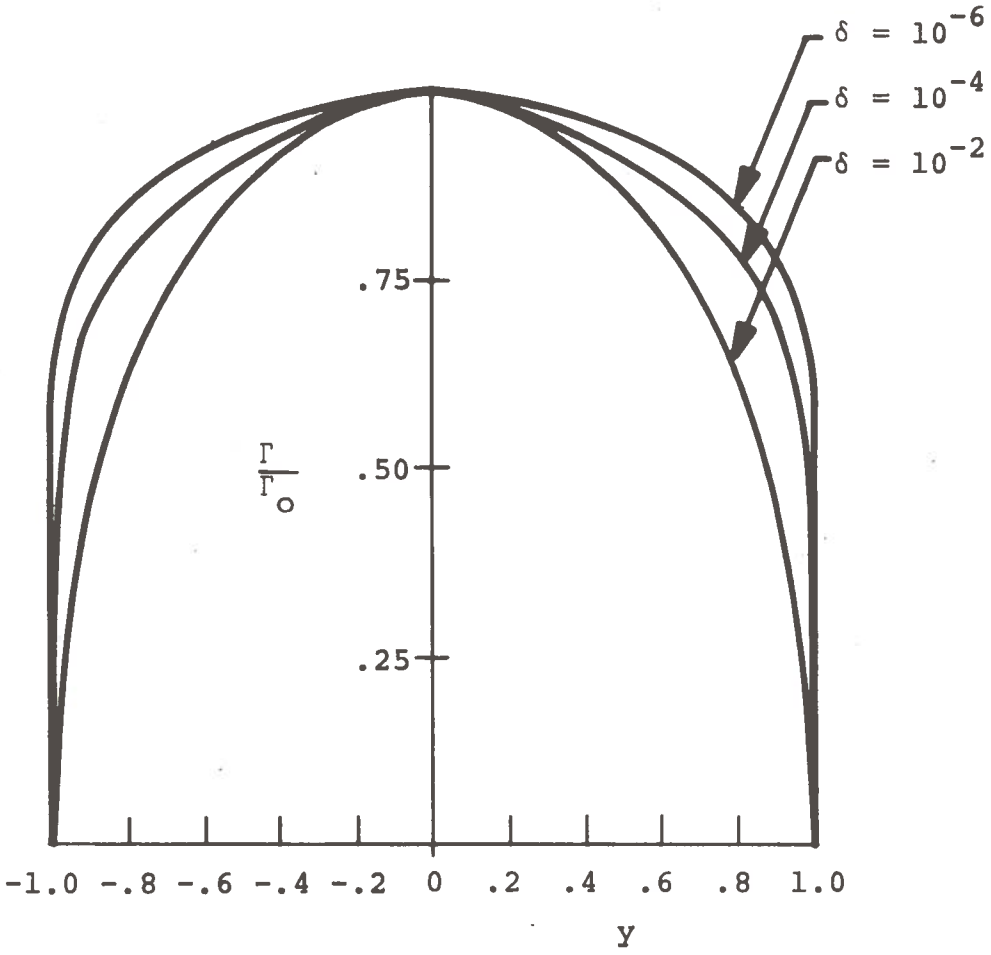

Figure A-4. Spanwise Distribution of Lift Normalized by the Lift at the Center. $\varepsilon = 0.1$

above an infinite ground plane, Fig. A-5, using conformal mapping. The configurations differ but the nature of the flow is similar for these two cases. He presents his results in terms of a drag factor σ, which is the inverse of the efficiency factor K. Fig. A-6 shows his results compared to (24) using the present notation. As can be seen, for small values of ε the agreement is quite good. Evidently for larger values of ε the differences in configuration become more significant.

A SOLUTION FOR THE FLOW UNDER THE WING

In this section we show how the Trefftz plane solution may be used to give an approximate expression for the flow under the wing itself. For this three dimensional problem a potential Φ is assumed to have a separable form:

$$\Phi(x,y,z) = m(x)\phi^{c}(y,z) \qquad (27)$$

That is, we assume that the flow in each cross sectional plane looks like the Trefftz plane flow calculated previously, with the magnitude m varying continuously with x from the leading edge to the trailing edge. The problem consists of solving for m(x). The linearized boundary conditions at the wing and on the ground are $w = \Phi_z = -\alpha$ at $z = 0$,

$w = 0$ at $z = -\varepsilon$.

The simplest solution for this is

$$w = \frac{-\alpha(\varepsilon+z)}{\varepsilon},$$

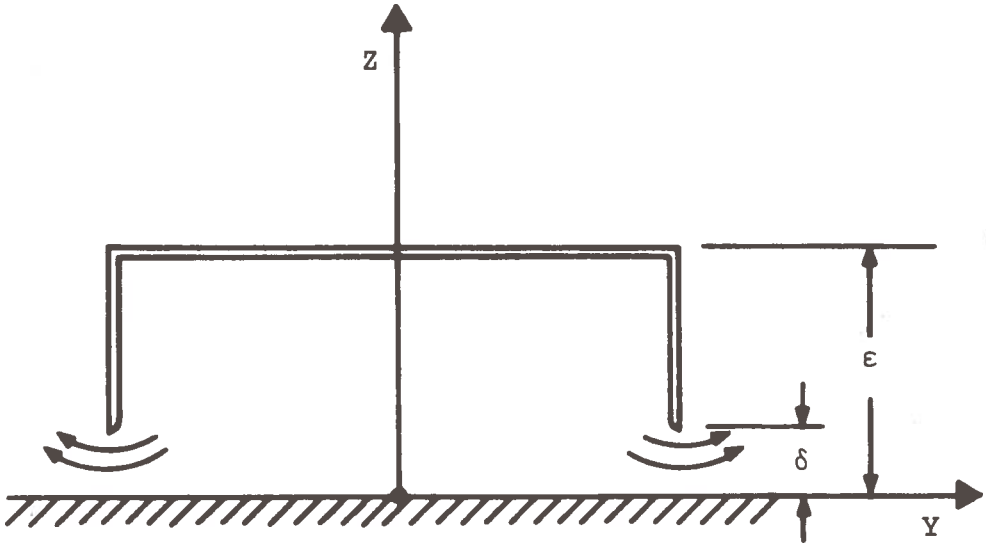

Figure A-5. Trefftz Plane of a Wing in Ground Effect Analyzed by Ashill (1970)

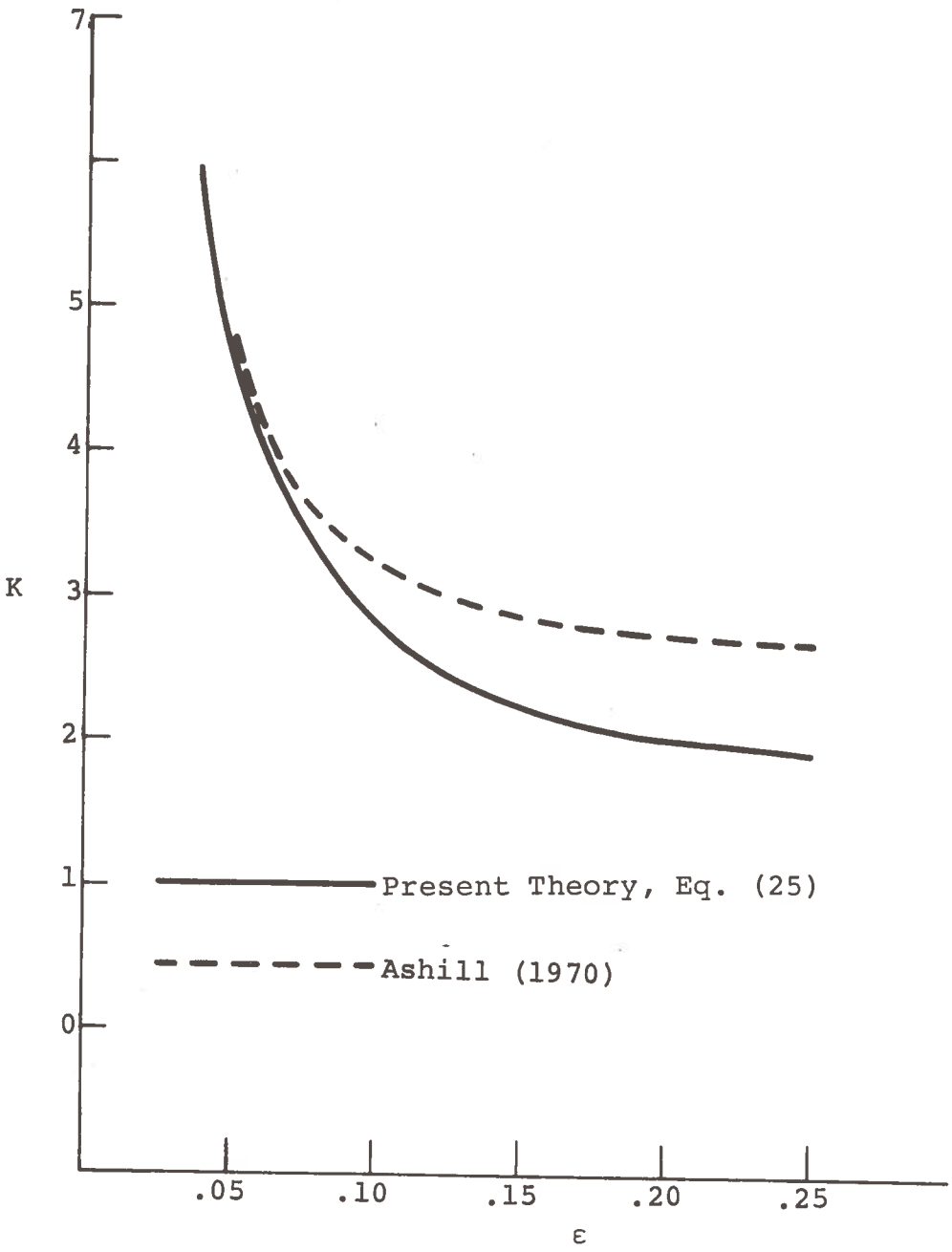

Figure A-6. Comparison of the Present Asymptotic Theory with Results Obtained Using Conformal Mapping for $\delta = .025$. K = Aspect Ratio Augmentation Factor Defined in Eq. (2).

which gives

$$\Phi_{zz} = - \frac{\alpha}{\varepsilon} \tag{28}$$

This equation is valid in the channel region under the wing, which excludes a narrow strip with a width of $0(\varepsilon)$ at each of the edges. Laplace's equation may be written

$$\Phi_{xx} + \Phi_{yy} = - \Phi_{zz} = \frac{\alpha}{\varepsilon} \tag{29}$$

which we propose to solve in the following fashion:

$$\Phi_{xx} = \alpha_1/\varepsilon \tag{30}$$

$$\Phi_{yy} = \alpha_2/\varepsilon \tag{31}$$

where

$$\alpha_1 + \alpha_2 = \alpha \ . \tag{32}$$

This formulation is based on a simple physical reckoning. The downwash flow which is being forced into the channel must either escape in the longitudinal direction out the leading and trailing edges, or it must move laterally out through the side edge gaps. These effects are associated with α_1 and α_2 respectively. It is proposed that a simple superposition of these two effects will give an accurate approximation for the flow.

Equation (31) is satisfied by choosing $\alpha_2 = m$, so that (32) becomes

$$\alpha_1 = \alpha - m \tag{33}$$

In order to satisfy (30) it is necessary to introduce the notion of an average value A for the potential ϕ^c:

$$A \equiv -\frac{1}{2}\int_{-1}^{+1} \phi^c\,(y,o)\,dy \tag{34}$$

This makes it possible to write (27) as follows

$$\Phi \cong -\,m(x)A \tag{35}$$

That is, for each chordwise station x, instead of using the actual value of ϕ^c, which varies with the spanwise position, the average value is used. In this manner a solution is obtained which has a correct average value at each station. Combining equations (30), (33), and (35) we obtain the governing equation for m:

$$m_{xx} - \frac{m}{A\varepsilon} = \frac{-\alpha}{A\varepsilon} \tag{36}$$

The boundary conditions on m are quite simple. At the trailing edge, which is most conveniently located at x = 0, the pressure coefficient must be zero

$$m_x = 0 \quad \text{at} \quad x = 0 \tag{37}$$

The potential at the leading and side edges must also be zero

$$m = 0 \quad \text{at} \quad x = -C \tag{38}$$

We obtain

$$m = \alpha\left[1 - \cosh \lambda x_c/\cosh \lambda\right], \tag{39}$$

where

$$\lambda \equiv c/\sqrt{A\epsilon} \quad , \tag{40}$$

and $x_c \equiv x/c$, the longitudinal position normalized by the chord (rather than the semispan). It is a straightforward matter to compute the lift coefficient using

$$C_L = \frac{2}{\text{Area}} \int_{-1}^{+1} \Phi\ (o,y,0)dy \quad . \tag{41}$$

After some manipulation the lift curve slope may be written

$$C_{L_\alpha} = \frac{\alpha}{\epsilon_c} f\ (\lambda) \tag{42}$$

where

$$f(\lambda) = \frac{2(\cosh \lambda - 1)}{\lambda^2 \cosh \lambda} \tag{43}$$

and $\epsilon_c \equiv \epsilon/c$, the height to chord ratio, which is the small parameter used in the two-dimensional theory of Widnall and Barrows (1970). The quantity λ thus emerges as another fundamental parameter for the present case. Using (34) to substitute for A in (40), we have

$$\lambda = c\left[\frac{1}{3} + \frac{2\epsilon}{\pi} \log \frac{4\epsilon}{\pi^2\delta^2}\right]^{-\frac{1}{2}} \tag{44}$$

In the limit as the side gap $\delta \to 0$, $f(\lambda) \to 1$, so that (42) in this limit gives the same result as the two-dimensional theory, as expected. Thus one can regard $f(\lambda)$ as a correction factor for the lift curve slope due to the side gaps.

Another even more interesting limit is the case of large chord, which is to say small aspect ratio. As $c \to \infty$, the lift coefficient drops off as c^{-1}, ε and δ being held constant. In other words no additional lift is generated as the chord is made longer and longer! A look at the pressure distribution reveals that all the lift is being generated in the forward portion of the wing, which is precisely what is predicted from classical slender body theory for a rectangular plate in a free stream. Once the crossplane flow is established near the leading edge, the remaining length of the wing merely passes through this plane without any pressure difference between the upper and lower surfaces.

For low aspect ratio, the effect on the lift of very small values of δ is quite dramatic. Consider a wing with an aspect ratio of one third ($c = 6$) and $\varepsilon = 0.1$. If δ is only 1% of the semispan, the lift drops to 4% of its two-dimensional value! This is indeed discouraging.

It is, of course, physically unrealistic to assume that the fluid can so easily negotiate the sharp turn at the wing tips. Undoubtedly some separation of the flow will occur, giving the pattern shown in Fig. A-7. In fact, in order to maximize the amount of lift from a ram wing it is probably desirable to deliberately promote separation of this type. This picture of the flow was first presented by Kaario (1959), and later extended by Gallington, Miller, and Smith (1971). For a preliminary

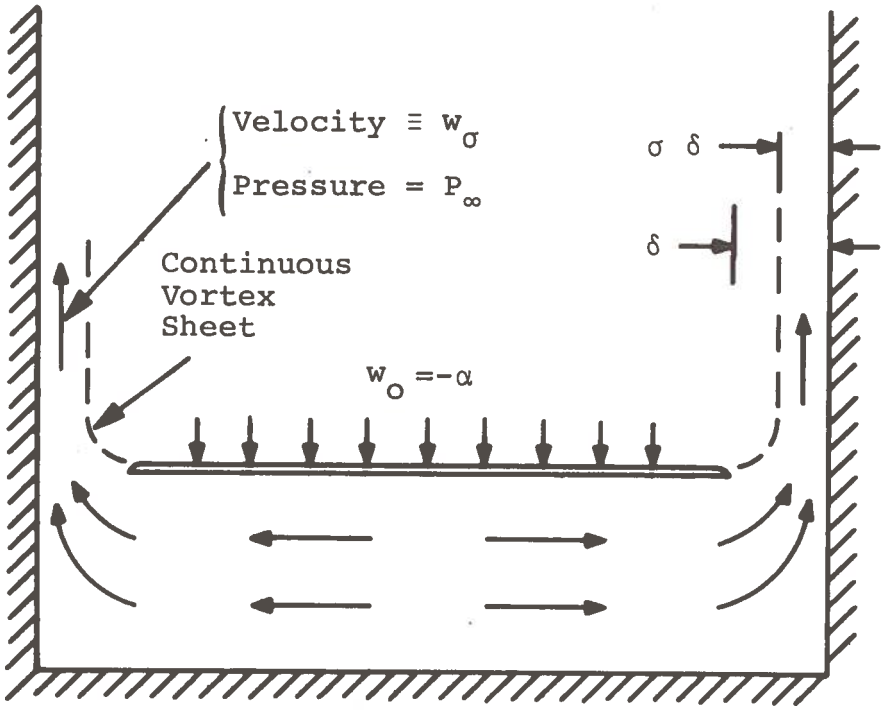

Figure A-7. Flow Separation at the Tips, Showing the Effect of Contraction

approach to analyzing this type of flow one can assume that the pressure at the point of smallest contraction is equal to the free stream value. It is also necessary to make some estimate of the contraction coefficient σ, which will depend on the precise geometric shape of the wingtip. Reasonable values of σ extend from 1.0 to 0.6.

The increased pressure in the channel due to tip vortex separation means that the velocity in the channel decreases. For a constant side gap this velocity u should be constant once separation is fully established. Hence the simplest flow model which accounts for the separation phenomena is one in which a uniform velocity decrease is superimposed on the potential flow solution. Note that a uniform velocity such as this does not effect mass continuity as expressed in (36).

For a free stream velocity of unity, the pressure condition at the contraction (Fig. A-7) reads

$$u^2 + w_\sigma^2 = 1 \tag{45}$$

Conservation of mass dictates that the volume flux into the channel equals the flux through the contraction:

$$\alpha u = \sigma\delta\, w_\sigma = \sigma\delta\,(1-u^2)^{\frac{1}{2}} \tag{46}$$

One can readily solve this equation for u and compute the pressure coefficient:

$$C_p = 1 - u^2 = \frac{\alpha^2}{\alpha^2+\sigma^2\delta^2} \tag{47}$$

Since this pressure is uniform under the entire wing, this value also gives the lift coefficient. Some modification of this solution is required near the trailing edge to allow free stream pressure to be obtained there; this will be left to a later report.

For small angles of attack this contribution to the lift is proportional to α^2, and may be added to the linearized potential flow contribution which is proportional to α. The latter may be associated with the pressure required to establish the cross plane flow, while the former comes from the pressure required to maintain this flow in the presence of viscous separation at the tips.

Experiments on a flat-bottomed rectangular wing in a trough have been conducted by Pepin (1970) using the method of images. This wing had a curved upper surface to prevent flow separation, and a maximum thickness of 3.75%. A comparison with the theoretical result obtained by adding (42), (47), and C_L for $\alpha = 0$ is shown in Fig. A-8. A value of 0.8 was used for σ. As can be seen, the agreement is reasonable, and the contribution from the α^2 term is very important even for extremely small angles of attack. Better agreement could be obtained with a more careful analysis of the unsteady flow effects on the contraction coefficient σ.

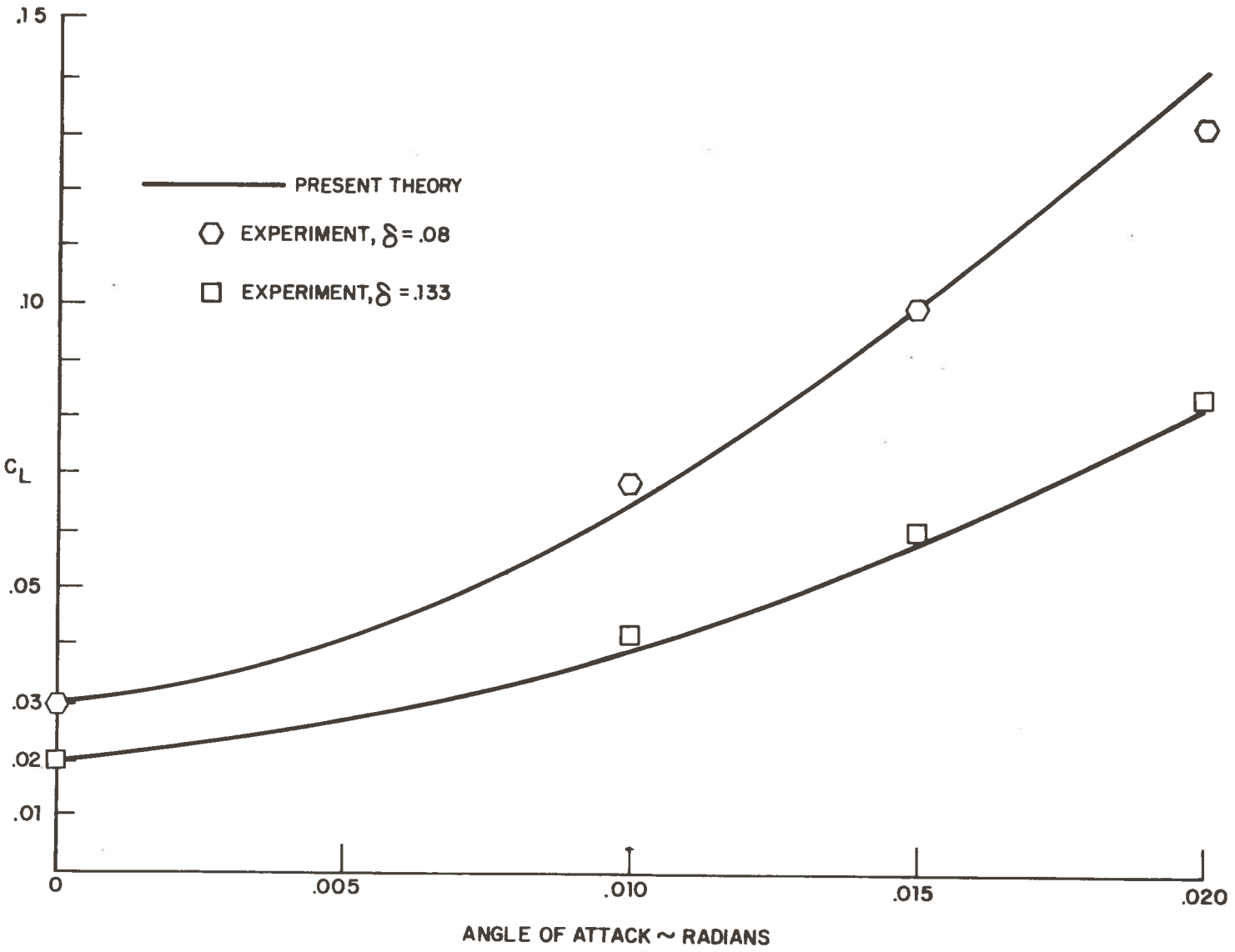

Figure A-8. Comparison Between Experiment and the Theoretical Values Obtained by Adding (42), (47) and C_L for $\alpha = 0$. The Leading Edge Clearance Ratio $\varepsilon = .21$ for all Cases. Aspect Ratio = 1/3.

APPENDIX B

A PRELIMINARY STUDY OF LATERAL STABILITY

APPENDIX B

A PRELEMINARY STUDY OF LATERAL STABILITY

It is, of course, difficult to begin a stability analysis for ram wing vehicles if the guideway cross-section is unspecified. Obviously specific configurations could be established and analyzed in some detail, but what is attempted here instead is the initiation of a process which will eventually show how to design a guideway which will yield the optimum lateral dynamic characteristics for the vehicle. Once this design is known a tradeoff can be made with the civil engineering aspects of the problem and an optimum system can be established.

The vehicle contour at the trailing edge must follow some symmetric curve $z = f(y)$ as shown in Fig. B-1. A spectrum of reasonable curves will range from circular to vee shaped to rectangular.

A circular guideway (or semicircular; whether or not the cross-section is closed over the top to form a tube has little bearing on the present discussion) has been mentioned as an attractive design due to the possibility that the vehicle can be made to bank like a togoggan through turns. It is also a good starting point in the spectrum of possible shapes since it inherently has the least roll stiffness (i.e. no roll stiffness about the center of the circle).

It is very useful to start with the problem first investigated by Frederick and Lee (1966) shown in Fig. B-2. The

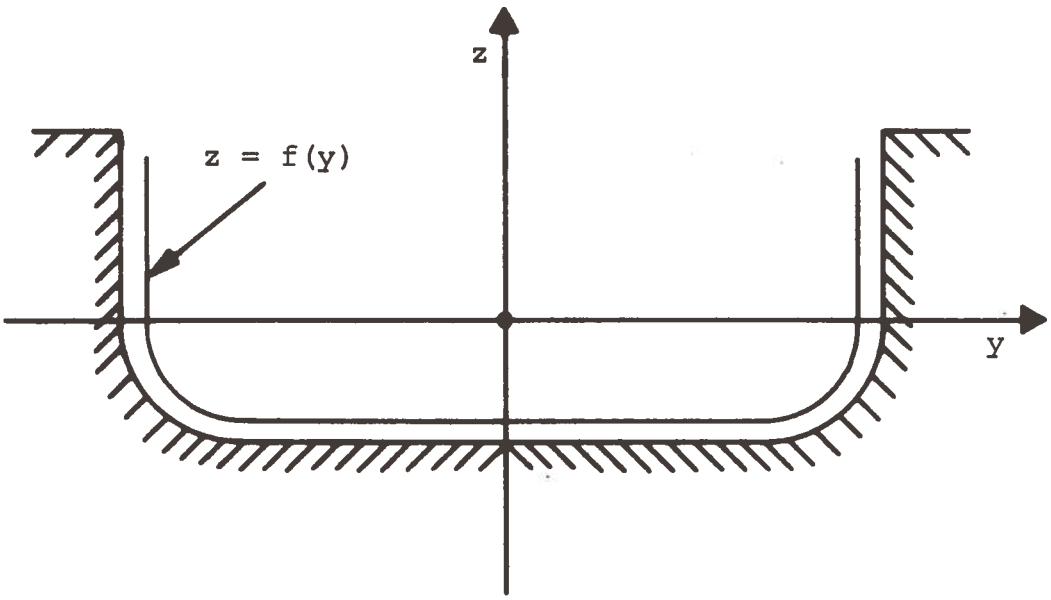

Figure B-1. Generalized Vehicle. The Function f(y) Describing the Bottom Contour of the Vehicle Might be Found from a Hypothetical Optimization Study.

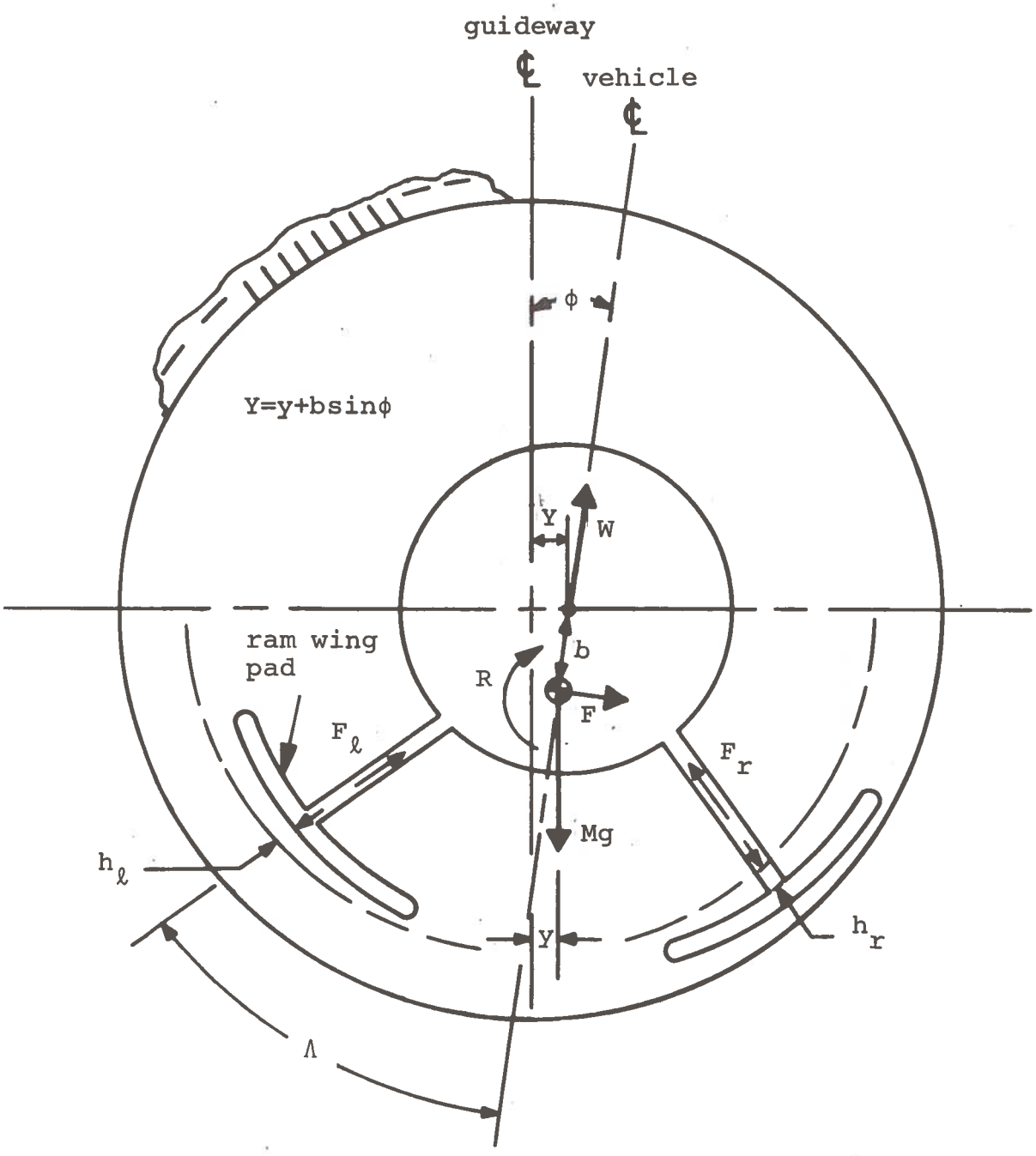

Figure B-2. Vehicle in a Circular Guideway First Studied by Frederick and Lee (1967)

example here is a cylindrical vehicle in a tube supported on two sets of pads, which may be either air cushions or ram wings; the only stipulation made about these pads is that their forces always act in the direction of the supporting struts. A rigorous formulation of the problem for five degrees of freedom may be found in the above reference, in this appendix a very abbreviated development will be given. We are here interested in the lateral dynamics so only yaw, side sway, and roll motions need be mentioned. Furthermore, the yaw motions of the vehicle have a secondary relationship with the cross-sectional geometry, inclusion of these motions in this analysis would only serve to confound the original purpose of the study: establishing desirable guideway features. In the design of the vehicle itself, of course, these motions must be included.

The equilibrium forces on the pads are just adequate to support the vehicle weight W, and the dynamic force for each pad is a linear function of h, the perturbation from equilibrium height. For the right pad we write

$$F_r = K_1 h_r + K_2 \dot{h}_r \qquad \text{(B-1)}$$

and similarly for the left pad.

The usual rotating coordinate system centered at the c.g. can be used to formulate this problem, but considerable simplification may be obtained by introducing the variable Y, which is the distance of the center of the vehicle from equilibrium:

$$Y = y + b \sin \phi \qquad \text{(B-2)}$$

where y is the perturbation of the c.g. from equilibrium, and b is the vertical distance from the center. Using the geometry of Fig. B-2 to calculate h_r and h_ℓ, and introducing the Laplace variable s, we can write the force on each pad:

$$F_r = (K_1+K_2s)\ Y \sin \Lambda \tag{B-3}$$

$$F_\ell = -\ (K_1+K_2s)\ Y \sin \Lambda \tag{B-4}$$

The resulting force and rolling moment at the c.g. become

$$R = b(F_\ell - F_r) \sin \Lambda \tag{B-5}$$

$$= 2b(K_1+K_2s)\ Y \sin^2 \Lambda$$

$$F = W\phi - 2(K_1+K_2s)\ Y \sin^2 \Lambda \tag{B-6}$$

Newton's relation may be used to equate F and R to the lateral and angular acceleration:

$$F = Ms^2y \tag{B-7}$$

$$R = Is^2\phi \tag{B-8}$$

Substituting from (B-2), (B-5), and (B-6) we obtain, after some rearrangement.

$$(s^2+sa_2+a_1)Y - (g+s^2b)\ \phi = 0 \tag{B-9}$$

$$b(sa_2+a_1)Y + sk_x^2\ \phi = 0 \tag{B-10}$$

where

$$a_1 \equiv 2\ K_1 \sin^2 \Lambda/M \tag{B-11}$$

$$a_2 \equiv 2\ K_2\ \sin^2\Lambda/M \qquad \text{(B-12)}$$

$$k_x \equiv \sqrt{I/M} = \text{radius of gyration} \qquad \text{(B-13)}$$

By setting the determinant formed by (B-9) and (B-10) equal to zero, we obtain the characteristic equation for the coupled oscillations. First it is useful to introduce the notion of the pendular frequency:

$$\omega_p \equiv \sqrt{g/b} \qquad \text{(B-14)}$$

This is the radian frequency at which a pendulum of length b will oscillate for small motions. The characteristic equation may be written

$$s^2(s^2+sa_2+a_1) + \frac{b^2}{k_x^2}(s^2+\omega_p^2)(sa_2+a_1) = 0 \qquad \text{(B-15)}$$

It can be shown that this is essentially the same as the result obtained by Frederick and Lee, who had an additional term due to aerodynamic forces on the vehicle body. The equation as written here, however, is suitable for analysis on a root locus plot, with b^2 being used as gain. Considerable insight can be obtained from such a plot even if the parameters in (B-15) are not specified precisely. For no gain (b=0) the roll and sway motions are uncoupled. This represents the situation in which the c.g. is at the vehicle center, so there is no roll stiffness giving a double pole at the origin. It can be

expected that the sway oscillations can be represented by an ordinary overdamped second order system, so that the two remaining poles lie on the negative real axis.

The root locus given by this hypothesis is shown in Fig. B-3. Increases in gain correspond to lowering the center of gravity, thus increasing the coupling. The most striking feature of this plot is that two unstable roots exist for all values of gain (this may also be shown using the Routh-Hurwitz criterion). After some reflection this is perhaps not so surprizing as might appear at first. With no coupling there is no roll stiffness, and with a high degree of coupling the vehicle operates like an undamped pendulum; all degrees of coupling between these extremes have a slight negative damping. This may be looked upon as an illustration of the difficulty of stabilizing one unstabilized degree of freedom through coupling with an entirely different mode of motion.

This type of instability is probably the easiest type to eliminate; the addition of roll damping is all that is required. Surprisingly, adding roll stiffness alone does very little to help the problem, it is still not possible to obtain damped roots through coupling with the sway motions. For good response to crosswind disturbances, however, both stiffness and damping are required for the uncoupled roll motions. Whether coupling will be beneficial or harmful in this situation remains unclear.

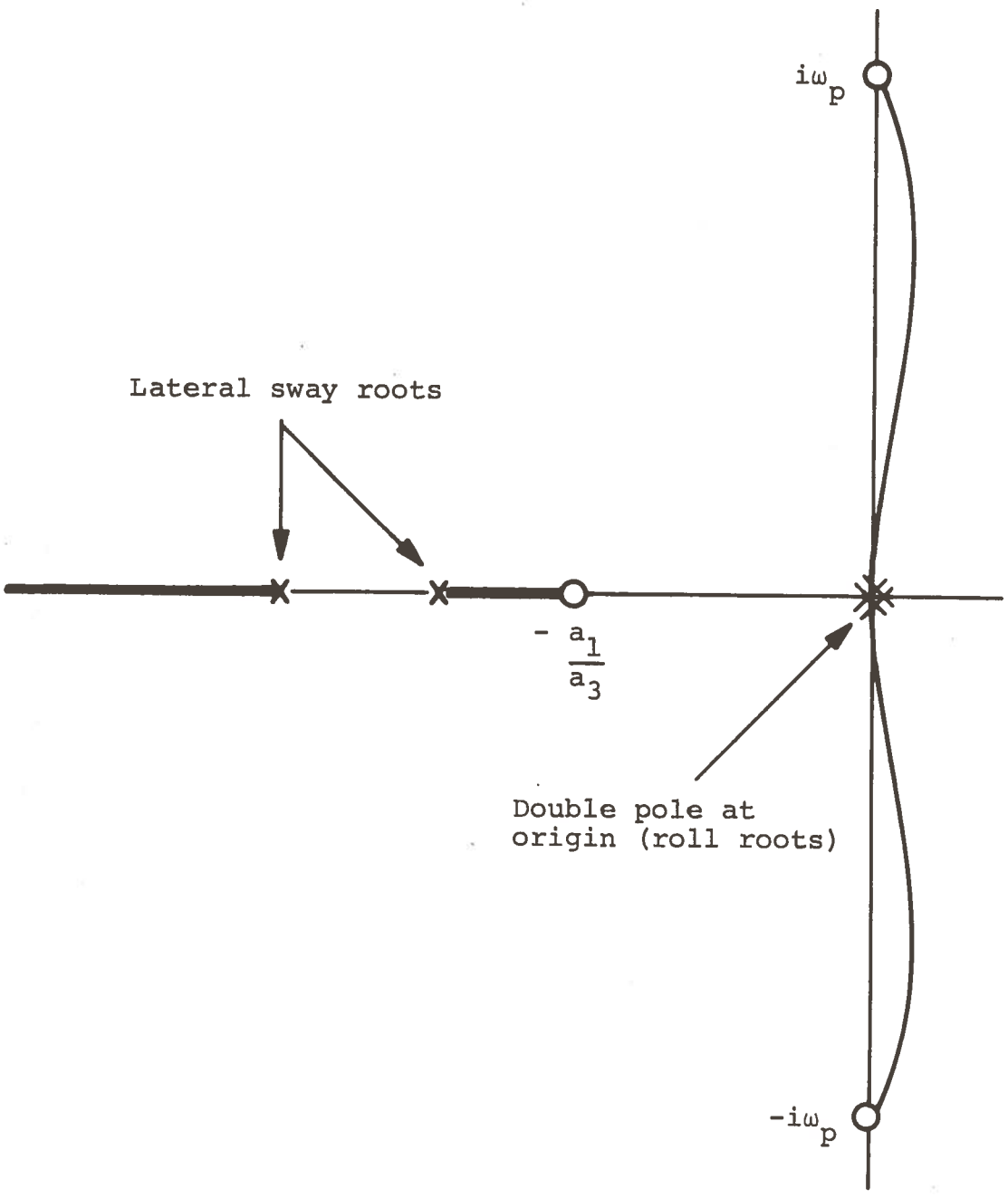

Figure B-3. Root Locus of the Vehicle in a Tube Calculated from (B-15). Gain ~ b^2

The reader may object that Fig. B-3 is not a true root locus since the zeros located at the pendular frequency will vary their location with gain. However, this does not effect any of the conclusions.

In the next stage of the guideway evolution it is useful to consider the vee guideway, Fig. B-4. There is no essential difference in the lateral dynamics between this and the circular case. As the vehicle rolls about the centerline each pad will exert a small restoring moment, which depends upon the pad width, but except for the case of very wide pads this effect cannot be expected to alter the basic character of the dynamic response. Since wide pads are inconsistent with the primary constraint of minimizing the guideway width, this design does not appear to offer much promise.

If a flat bottom is added to the vee, it becomes a trough with sloping sides, Fig. B-5. This is definitely a favorable step in the evolution of the guideway. The angulated pads can produce forces which directly contribute to the roll damping and roll stiffness. It can intuitively be seen that these forces increase with Λ, the angle of the sides. Unfortunately, however, the nature of the pressure distribution on such angulated pads is not known and very little of a quantitative nature can be said about this design at this time. Hopefully the analysis in Appendix A can be further developed to the point where such information can be provided. Quantitatively it can

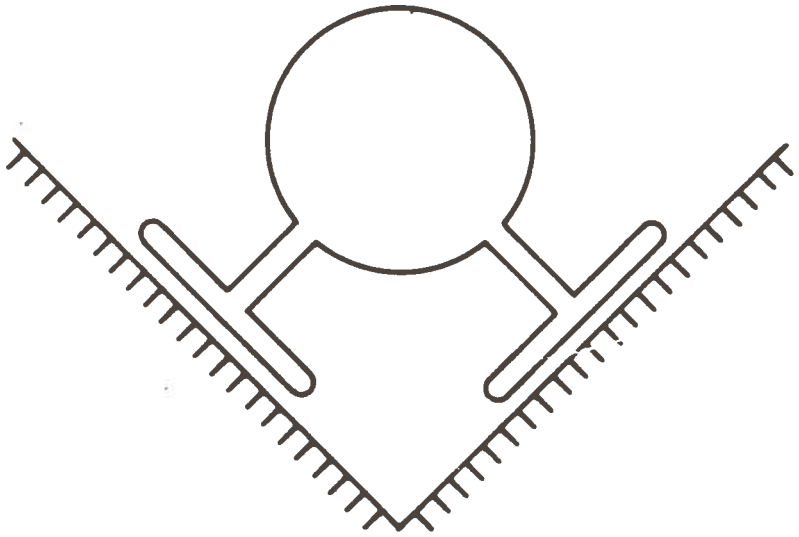

Figure B-4. The Vee Guideway has Lateral dynamic Characteristics Similar to the Circular Guideway

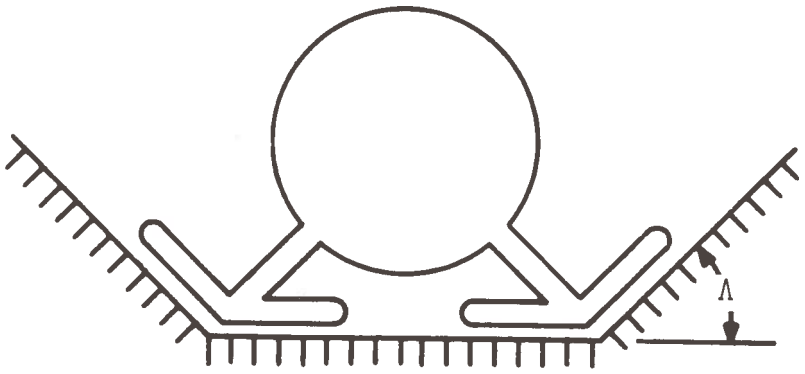

Figure B-5. The Addition of a Flat Bottom to the Guideway Improves the Roll Stability

be said that if Λ is chosen large enough the system will eventually have enough damping to become stable. A maximum practical limit on Λ is 90°, in which case we have a rectangular trough.

The configuration in Fig. B-5 is fairly close to the actual shape used in the glide tests. All that is required is to expand the vehicle body so that it completely fills in the space between the pads, giving an integrated lifting shape. The high speed films of these tests definitely confirm that the vehicle dynamic characteristics are of the same class as we have been discussing: good stability for the sway motions but poor damping for the roll oscillations. Whether the damping is positive or negative is unclear from both a theoretical and experimental standpoint. The theory has the above mentioned lack of development and the glide tests were too short (50 feet) to observe whether the roll oscillations were self-generating or caused by the impulse from the catapult.

In summary it can be seen that certain characteristics prevail among the various designs considered, and that roll motions will be a problem if the guideway width is constrained. Attention should be focused on those designs which produce a maximum of roll stiffness and damping for a given amount of width. Future research in lateral stability should be aimed at obtaining the important cross-coupling derivatives such as roll due to side sway and side force due to rolling.

APPENDIX C

EXPERIMENTAL RESULTS OF THE GLIDE TESTS

APPENDIX C

EXPERIMENTAL RESULTS OF THE GLIDE TESTS

Although the glide tests described in chapter two provide a convincing demonstration of a ram wing in action, it is very difficult to obtain quantitative data from this type of experiment. The only parameter which can be easily obtained is the lift coefficient, which can be calculated from a simple measurement of velocity. All the tests conducted had a lift coefficient of approximately 0.7, based on the planform of the main wing, which is comparable to what might be expected for a full scale vehicle (perhaps a bit high).

A typical output trace from the guideway instrumentation is shown in Fig. C-1. Three such traces were recorded at separate points along the track for each test, using an oscillograph recorder having a chart speed of 80 inches per second. The velocity of the model could thus be obtained at three points by measuring the width of each output trace.

The angle of the canard, α_c, could be varied continuously, and in the present series of tests one purpose was to note the effect of these variations on the flying characteristics. In Fig. C-2 the velocity is shown as a function of α_c. The ordinate is greatly magnified to show the differences in velocity at the three stations. Station number one is located uppermost, station two in the middle, and station three is near the lower end of the track. No significant observation can be made about

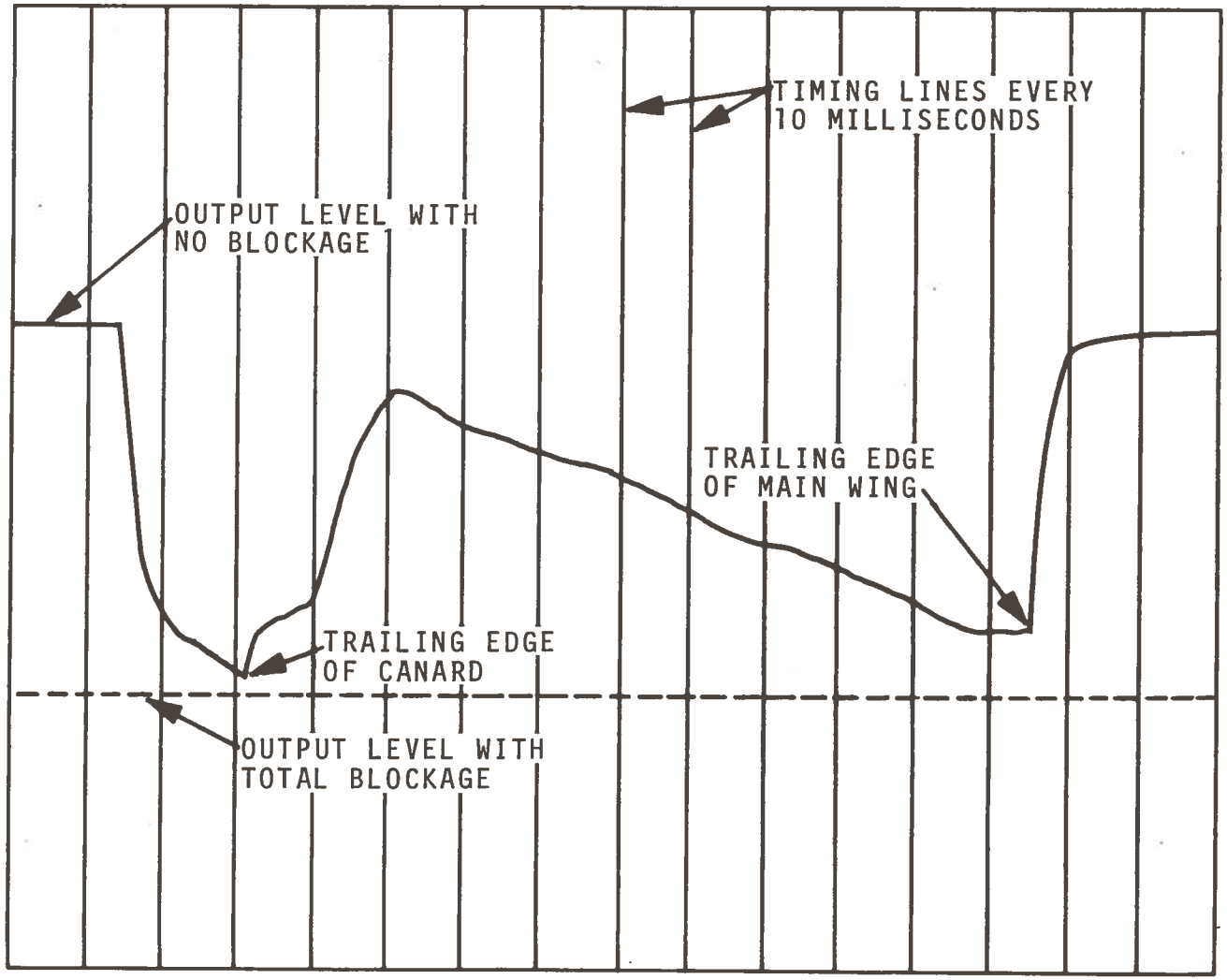

Figure C-1. Oscillograph Output Trace.

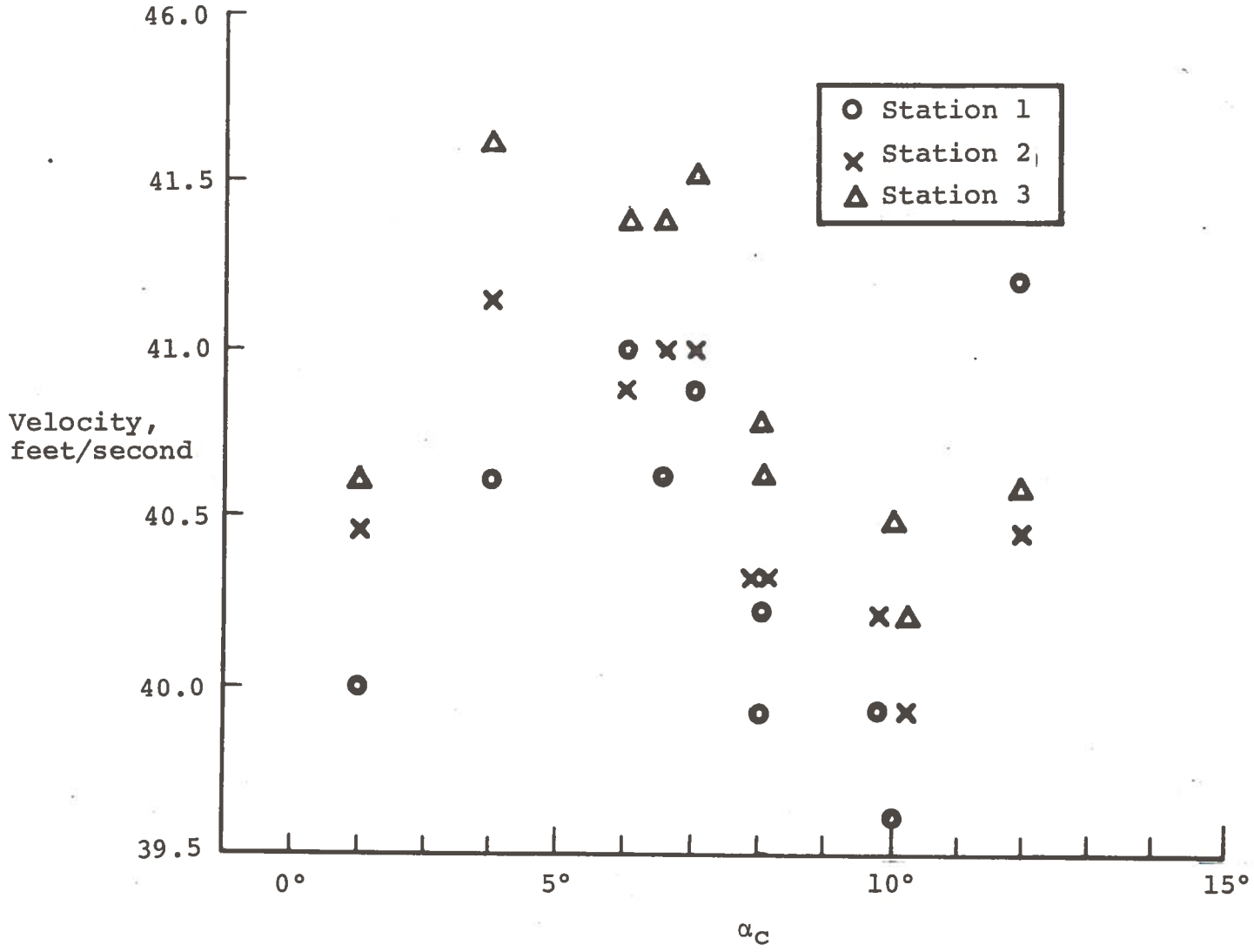

Figure C-2. Measured Velocity as a Function of α_c at Three Stations on the Guideway

the effect of α_c because of the scatter of the data, which is undoubtedly mostly due to variations in the starting impulse given by the catapult. Even though all the velocity measurements were consistent to within a few percent, accelerations calculated by taking differences in velocity showed a wide variation. With the angle of the track set at 1 in 9, accelerations measured in this manner ranged from 0.45 to 1.84 feet/sec^2. To reconcile these large differences a more accurate method for utilizing the oscilligraph data was developed.

It is apparent that an alternative method for obtaining velocity is to measure the time required for the model to pass from one station to the next (rather than the time required to pass by one station). Since the distance between stations is much greater than the length of the model, this second method is more accurate.

Let

v_1 = Velocity at station one

v_2 = Velocity at station two

v_{12} = Velocity measured between one and two.

A weighted average velocity U for the upper half of the track was defined as follows:

$$U = \frac{1}{4} (v_1+v_2+2v_{12}).$$

That is, V_{12} was given twice the weight of the other measurements since it was considered to be more accurate. A similar averaged velocity V for the lower half of the track

was also computed:

$$V = \frac{1}{4} (v_2 + v_3 + 2v_{23}).$$

The acceleration A was calculated by taking the difference

$$A = \frac{V-U}{\Delta t}$$

The acceleration computed in this manner is shown in Fig. C-3 as a function of α_c. Except for two data points, all values of A lie within 10% of one foot per second squared. With acceleration known, a simple computation gives the lift drag ratio:

$$\frac{L}{D} = \frac{1}{\tan \gamma - (A/g \cos \gamma)}$$

where $\tan \gamma$ = glide slope = 1/9. We obtain

$$\frac{L}{D} = 12.7$$

As a check on this value the slope of the track was changed to 1/13. No acceleration could be detected at this angle, indicating that this represents the actual ratio of drag to lift, within a few percent.

The functional relationship between α_c and drag is somewhat indirect, and it is perhaps not surprising that no change in L/D due to α_c could be detected in these tests. Increasing α_c causes a nose up moment which increases the angle of attack and equilibrium height of the model. This in turn will theoretically increase the induced drag which should cause the model to

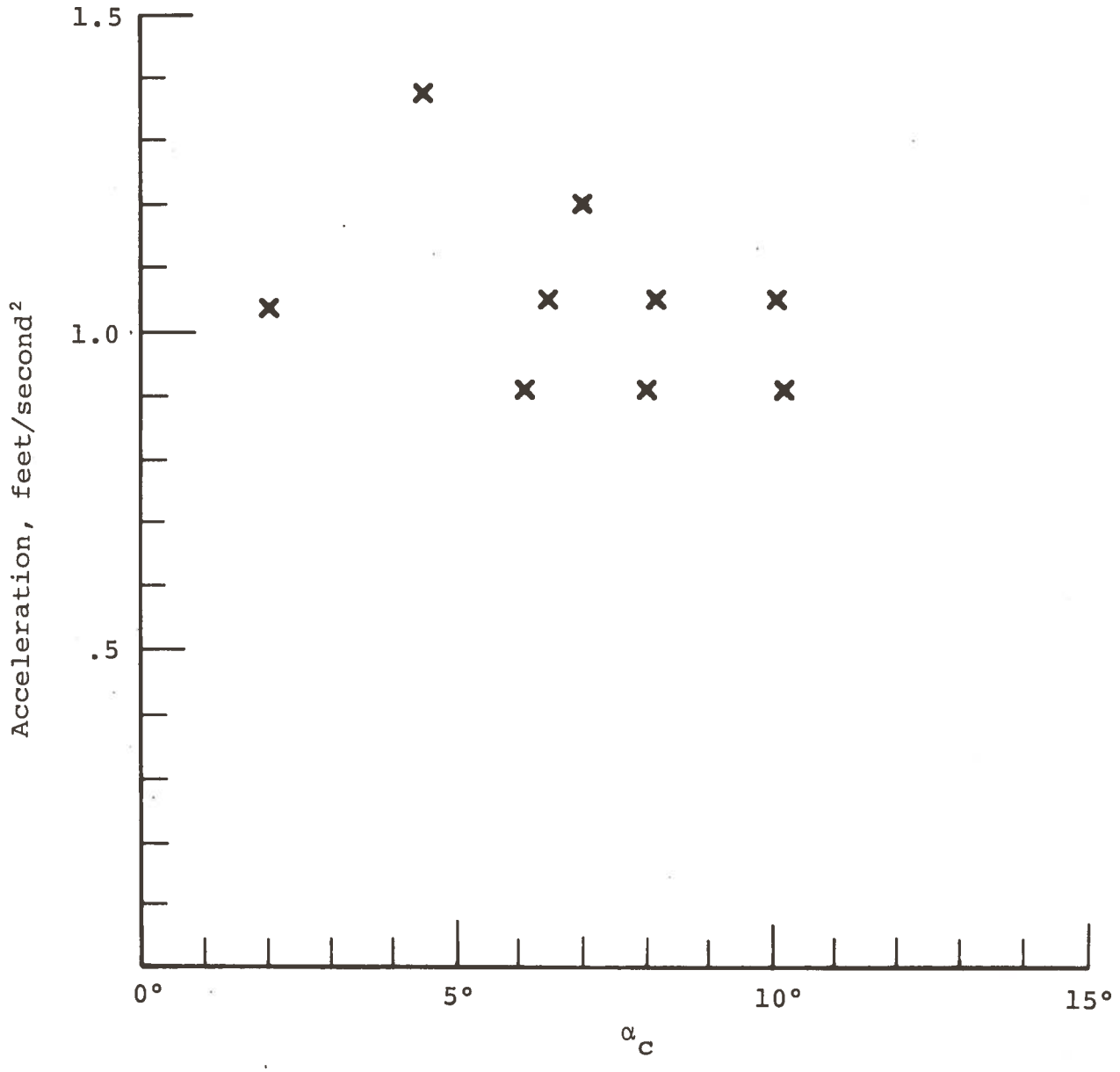

Figure C-3. Acceleration Calculated using the Weighted Average Method. Glide Slope = 1/9.

decelerate. Under favorable circumstances it would be more logical to observe these effects by measuring the height and angle of attack directly. However, the rolling motion of the model introduced so much uncertainty into these measurements that no significant results could be obtained from them. Fig. C-4 shows uncorrected data for the height at the trailing edge. The optical system responds to the height of the lowest point on the model, so that if there is a small roll angle the height output will read somewhat lower than it would if the model were in a level position. The roll angles shown in Fig. 2-3 are approximately $\pm$ 3°. The semispan of the bottom surface of the model is 5", so the maximum error in height is 5" x tan 3° = 0.26". Since a maximum readout for the height is recorded if the model is in a level position, we can expect that the maximum values shown in Fig. C-4, 0.6", give the approximate height of the trailing edge when the model is level, and all other values correspond to various degrees of rolling. Note that all the values shown fall within the maximum error calculated above. Thus we may conclude that the center point of the trailing edge normally flies at 0.6", and roll angles are 3° or less. It is also apparent that very little further information will come from the height data until either the roll oscillations are eliminated or a method is developed to record roll angles so that proper corrections can be made to these measurements.

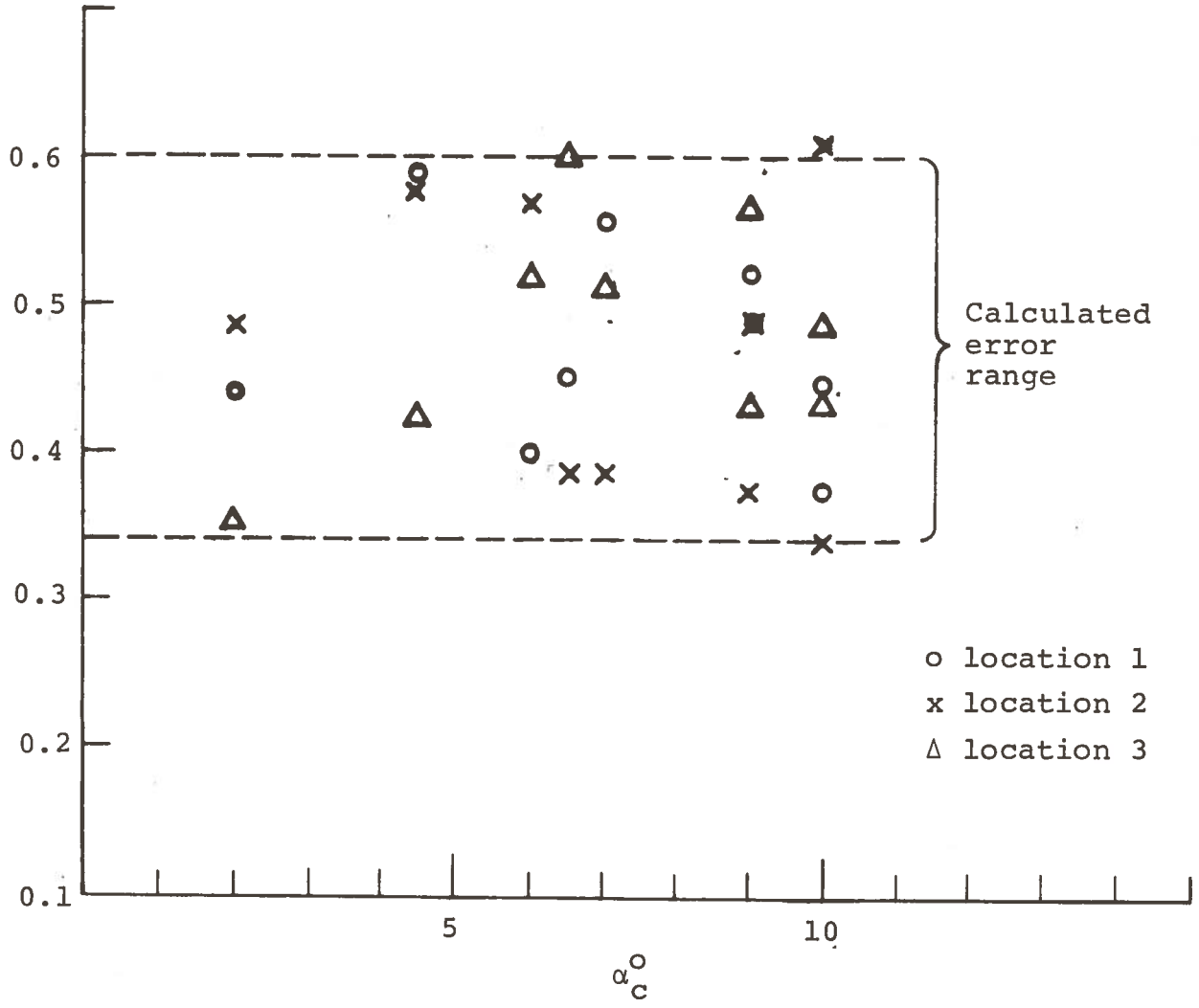

Figure C-4. Trailing Edge Clearance in Inches as a Function of α_c. The Error Range Shown is for a $\pm 3°$ Roll

A qualitative conclusion which may be drawn is that there is no dramatic change in the flight attitude of the model as α_c is varied. This is an indication that the selected design using a canard followed by main body provides an adequate margin of longitudinal stability. We may expect that a vehicle design which has a lower aspect ratio will have even greater pitch stability, in which case it might be possible to dispense with the canard; this would further simplify the ram wing in comparison to alternative concepts for high speed ground transportation.